Theoretical study of neutrino-induced coherent pion production off nuclei at T2K and MiniBooNE energies

J. E. Amaro,[1] E. Hernández,[2] J. Nieves,[3] and M. Valverde[1,4]

[1]*Departamento de Física Atómica, Molecular y Nuclear, Universidad de Granada, E-18071 Granada, Spain*
[2]*Grupo de Física Nuclear, Departamento de Física Fundamental e IUFFyM, Facultad de Ciencias, E-37008 Salamanca, Spain*
[3]*Instituto de Física Corpuscular (IFIC), Centro Mixto CSIC-Universidad de Valencia, Institutos de Investigación de Paterna, Aptd. 22085, E-46071 Valencia, Spain*
[4]*Department of Subatomic and Radiation Physics, Ghent University, Proeftuinstraat 86, B-9000 Gent, Belgium*

(Received 10 November 2008; published 7 January 2009)

We have developed a model for neutrino-induced coherent pion production off nuclei in the energy regime of interest for present and forthcoming neutrino oscillation experiments. It is based on a microscopic model for pion production off the nucleon that, besides the dominant Δ pole contribution, takes into account the effect of background terms required by chiral symmetry. Moreover, the model uses a reduced nucleon-to-Δ resonance axial coupling, which leads to coherent pion production cross sections around a factor of 2 smaller than most of the previous theoretical estimates. In the coherent production, the main nuclear effects, namely, medium corrections on the Δ propagator and the final pion distortion, are included. We have improved on previous similar models by taking into account the nucleon motion and employing a more sophisticated optical potential. As found in previous calculations the modification of the Δ self-energy inside the nuclear medium strongly reduces the cross section, while the final pion distortion mainly shifts the peak position to lower pion energies. The angular distribution profiles are not much affected by nuclear effects. Nucleon motion increases the cross section by $\sim$15% at neutrino energies of 650 MeV, while Coulomb effects on charged pions are estimated to be small. Finally, we discuss at length the deficiencies of the Rein-Sehgal pion coherent production model for neutrino energies below 2 GeV, and, in particular, for the MiniBooNE and T2K experiments. We also predict flux-averaged cross sections for these two latter experiments and K2K.

DOI: 10.1103/PhysRevD.79.013002 PACS numbers: 25.30.Pt, 12.15.−y, 12.39.Fe, 13.15.+g

I. INTRODUCTION

Neutrino-induced one-pion production off nucleons and nuclei in the intermediate energy region is a source of relevant data on hadronic structure. Pions are mainly produced through resonance excitation and these reactions can be used to extract information on nucleon-to-resonance axial transition form factors. Besides, a proper understanding of these processes is very important in the analysis of neutrino oscillation experiments. For instance, π^0 production by neutral currents (NC) is the most important ν_μ-induced background to experiments that measure $\nu_\mu \to \nu_e$ oscillations in the neutrino energy range around 1 GeV [1]. This is because NC π^0 events can mimic ν_e signal events when, for example, one of the two photons associated with the $\pi^0 \to \gamma\gamma$ decay is not detected. This can happen when a photon exits the detector before showering or does not have enough energy to initiate a shower. Similarly, π^+ production by charged currents (CC) is an important source of background in $\nu_\mu \to \nu_x$ disappearance searches [2].

In reactions on nuclei, pions can be produced incoherently or coherently. In the latter case the nucleus remains in its ground state. Coherent reactions are controlled by the nucleus form factor and are more forward peaked than incoherent ones. CC coherent pion production has been studied at higher energies in a number of experiments [3–8]. The results could be satisfactorily explained by the Rein-Sehgal model [9], which is based on the partially conserved axial current (PCAC) hypothesis [10]. The K2K Collaboration has recently conducted a search for CC coherent pion production induced by muon neutrinos with a mean beam energy of 1.3 GeV [11]. Contrary to expectations, they found no evidence for CC coherent pion production, setting an upper limit of 0.60% for the coherent to total CC pion production ratio. The data show a deficit of forward muons in the kinematical region where a sizable coherent production is expected. An attempt to explain this deficit has been done by Rein and Sehgal in Ref. [12] by including in their model the usually neglected finite muon mass effect [13,14]. In this way they find a 25% suppression caused by the destructive interference between the axial vector and pseudoscalar (pion-pole) amplitudes, reducing in this way the discrepancy between theory and experiment, though it still persists. This correction affects only CC processes and its relevance is reduced as the neutrino energy increases [12]. The negative K2K results are consistent with a very recent search performed by the SciBooNE Collaboration [15].

NC coherent pion production was observed by the Aachen-Padova group [16] on a ^{27}Al target with both the muon neutrino and antineutrino CERN PS beam with

average energy of 2 GeV. Positive evidence was also seen by the PS-Gargamelle neutrino and antineutrino Freon experiments [17]. Very recently, the MiniBooNE Collaboration announced the first observation of NC coherent π^0 production below 2 GeV [18]. When integrated over the MiniBooNE flux, they find a ratio of coherent plus diffractive production over all exclusive NC π^0 production given by $19.5 \pm 1.1(\text{stat.}) \pm 2.5(\text{sys.})\%$ for a mineral oil target (CH_2). By using Monte Carlo they estimate the coherent rate for a pure ^{12}C target to be $20.3 \pm 2.8(\text{stat.})\%$.

On the theoretical side the Rein-Sehgal model [9] mentioned above assumes that coherent pion production is dominated by the divergence of the axial current [19–22] and can thus be related to the pion-nucleus coherent scattering via PCAC. Extrapolation to nonforward angles is done by including a propagator term $(1 + Q^2/m_A^2)^{-2}$ with $m_A \approx 1$ GeV. The effects on the model of considering a finite muon mass was recently analyzed in Refs. [12,14] and, as stated above, they give rise to a 25% reduction of the CC coherent pion production by muon neutrinos at low neutrino energies. However, one should note that the Rein-Sehgal model does not account for nuclear pion absorption, since it does not consider two body mechanisms which are those responsible for the absorption of the outgoing pions, and it does not correctly treat quasielastic collisions either. Besides, the corrections to the outgoing pion angular dependence predicted by the model become quite important for the low neutrino energies relevant in MiniBooNE and T2K experiments, as we will show in Sec. IV B.

The PCAC approach was also used in the models of Refs. [23–27]. In Ref. [27] the authors take into account the muon mass effect and include a small non-PCAC transverse current contribution. In all cases the distortion of the final pion was included. There are other approaches that do not rely on PCAC. In Ref. [28] coherent pions are produced by virtual Δ-h excitations in the nucleus. The model includes the modifications of the nucleon and Δ propagators in the medium, evaluated in a relativistic mean field approximation, but no final pion distortion was taken into account. Kelkar *et al.* [29] improve on the above calculation by doing a more sophisticated evaluation of the Δ self-energy in the medium and treating the final pion distortion in a realistic way by solving the Klein-Gordon (KG) equation for a pion-nucleus optical potential. The model of Ref. [30] uses similar medium corrections and improves on the description of the elementary reaction. On the other hand the final pion distortion is treated in the eikonal approximation which is known to fail at low pion energies. In Refs. [31,32] the authors follow the Kelkar *et al.* calculation in the treatment of the final pion distortion while using, as in Ref. [30], a more complete and fully relativistic elementary amplitude.

In a recent publication we have developed a model for CC and NC neutrino- and antineutrino-induced pion production off the nucleon in the intermediate energy region [33], which represents the natural extension of that developed in Ref. [34] for the electron analogue $eN \to e'N'\pi$ reaction. Most previous studies [35–43] of these processes considered only the dominant Δ pole mechanism in which the neutrino excites a $\Delta(1232)$ resonance that subsequently decays into $N\pi$. In our model we have also included background terms required by chiral symmetry (see Fig. 1 below). Some background terms were considered before in the works of Refs. [44–46] although none of these models was consistent with chiral counting. In Ref. [33], we found that background terms produced significant effects in all channels. As a result we had to readjust the strength of the dominant Δ pole contribution. The least known ingredients of the model are the axial nucleon-to-Δ transition form factors, of which C_5^A gives the largest contribution. This strongly suggested the readjustment of that form factor to the experimental data, which we did by fitting the flux-averaged $\nu_\mu p \to \mu^- p \pi^+$ Argonne National Laboratory (ANL) q^2-differential cross section for pion-nucleon invariant masses $W < 1.4$ GeV [47,48]. Our full model, thus obtained, leads to an overall better description of the data for different CC and NC, neutrino- and antineutrino-induced, one-pion production reactions off the nucleon. This reduction of the $C_5^A(0)$ value is consistent with recent results in lattice QCD [49], quark model [50] and phenomenological studies [51].

Here, we shall apply our model to evaluate CC and NC coherent pion production in nuclei, including the chiral background terms in the elementary amplitude. We follow a scheme similar to that advocated in Refs. [31,32],[1] but improving the results of these latter references by properly taking into account the motion of the nucleons and correcting for some numerical inaccuracies that affected the calculations of these two references [52]. Our model should work better close to threshold, and hence we will concentrate in the neutrino energy range of MiniBooNE and the future T2K experiment where the neutrino peak energy is expected to be around $0.6 \div 0.7$ GeV [53]. This work is organized as follows: in Sec. II we discuss our model for the evaluation of CC coherent pion production, including the most relevant aspects of medium corrections for the Δ and the evaluation of the final pion distortion. In Sec. III we find the corresponding expressions for the NC coherent pion production case. Finally, in Sec. IV we present and discuss our results.

II. CC NEUTRINO AND ANTINEUTRINO-INDUCED REACTIONS

We will focus on the coherent CC pion production reaction induced by neutrinos,

$$\nu_l(k) + A_Z|_{gs}(p_A) \to l^-(k') + A_Z|_{gs}(p'_A) + \pi^+(k_\pi). \quad (1)$$

The process consists of a weak pion (π^+) production

followed by the strong distortion of the pion in its way out of the nucleus. In the coherent production the nucleus is left in its ground state by contrast with the incoherent production where the nucleus is either broken or left in some excited state.

The unpolarized differential cross section, with respect to the outgoing lepton and pion kinematical variables, is given in the Laboratory (LAB) frame by

$$\frac{d^5\sigma_{\nu_l l}}{d\Omega(\hat{k}')dE'd\Omega(\hat{k}_\pi)} = \frac{|\vec{k}'|}{|\vec{k}|}\frac{G^2}{4\pi^2}L^{(\nu)}_{\mu\sigma}W^{\mu\sigma}_{\mathrm{CC}\pi^+} \qquad (2)$$

with $\vec{k}$ and $\vec{k}'$ the LAB lepton momenta, $E' = (\vec{k}'^2 + m_l^2)^{1/2}$ and m_l the energy and the mass of the outgoing lepton, $G = 1.1664 \times 10^{-11}$ MeV^{-2} the Fermi constant, $\vec{k}_\pi$ and $E_\pi = (\vec{k}_\pi^2 + m_\pi^2)^{1/2}$ the LAB momentum and energy of the outgoing pion, and L and W the leptonic and hadronic tensors, respectively. The leptonic tensor is given by (in our convention, we take $\epsilon_{0123} = +1$ and the metric $g^{\mu\nu} = (+,-,-,-)$):

$$L^{(\nu)}_{\mu\sigma} = k'_\mu k_\sigma + k'_\sigma k_\mu - g_{\mu\sigma}k\cdot k' + i\epsilon_{\mu\sigma\alpha\beta}k'^\alpha k^\beta, \qquad (3)$$

and it is not orthogonal to the transferred four-momentum $q = k - k'$ even for massless neutrinos, i.e., $L^{(\nu)}_{\mu\sigma}q^\mu = -m_l^2 k_\sigma$.

The hadronic tensor includes all the nuclear effects and it can be approximated by

$$W^{\mu\sigma}_{\mathrm{CC}_{\pi^+}} = \frac{|\vec{k}_\pi|}{64\pi^3 M^2}\mathcal{A}^\mu_{\pi^+}(q,k_\pi)(\mathcal{A}^\sigma_{\pi^+}(q,k_\pi))^* \qquad (4)$$

$$\mathcal{A}^\mu_{\pi^+}(q,k_\pi) = \int d^3\vec{r}\, e^{i(\vec{q}-\vec{k}_\pi).\vec{r}}\{\rho_p(\vec{r})[\mathcal{J}^\mu_{p\pi^+}(\vec{r};q,k_\pi)] + \rho_n(\vec{r})[\mathcal{J}^\mu_{n\pi^+}(\vec{r};q,k_\pi)]\} \qquad (5)$$

with M the nucleon mass, $\rho_{p(n)}$ the nuclear proton (neutron) density, normalized to the number of protons (neutrons). Since we have neglected the recoil energy of the final nucleus we have $q^0 = k^0_\pi (\equiv E_\pi)$. Finally $\mathcal{J}^\mu_{N\pi^+}(\vec{r};q,k_\pi)$ stands for the nucleon helicity averaged $W^+N \to N\pi^+$ amplitude evaluated inside the nuclear medium as explained below. Our model for the coherent nuclear process is built up from the coherent scattering of the W^+ boson with each of the nucleons of the nucleus producing an outgoing π^+. The nucleon state (wave function) remains unchanged in the dispersion, and thus after summing over all nucleons we obtain the nuclear densities which appeared in the hadronic tensor $W^{\mu\sigma}_{\mathrm{CC}\pi^+}$ of Eq. (4). In the elementary $W^+N \to N\pi^+$ process, energy conservation is accomplished by imposing $q^0 = E_\pi$, while the transferred momentum $\vec{q} - \vec{k}_\pi$ has to be accommodated by the nucleon wave functions. Thus, the coherent pion production process is sensitive to the Fourier transform of the nuclear density for momentum $\vec{q} - \vec{k}_\pi$ (see Eq. (5)) This nuclear form factor gets its maximum value when $\vec{q}$ and $\vec{k}_\pi$ are parallel, but for this particular kinematics the vector contribution of the $\mathcal{J}^\mu_{N\pi}$ amplitudes, which is purely transverse $\vec{k}_\pi \times \vec{q}$, vanishes. This is the reason why for electron and photon induced reactions, the coherent pion production cross section turned out to be a quite small fraction of the total inclusive nuclear absorption one [54,55]. For neutrino-induced reactions, the axial contribution of the amplitudes is not suppressed for kinematics where $\vec{q}$ and $\vec{k}_\pi$ are almost parallel. Thus, the reduction induced by the nuclear form factor is much less important, and one might expect a larger relative contribution of the coherent pion production channel, as it is the case for some purely hadron reactions (for instance, coherent pion production in the (^{3}He, t) in nuclei [56]). This dominance of the axial contributions has been extensively exploited, through the PCAC hypothesis, to relate the neutrino coherent pion production cross section with the pion-nucleus elastic differential one [9,12,27].

For the elementary process we have used the model recently derived in Ref. [33]. In addition to the Δ pole (ΔP) mechanism (weak excitation of the $\Delta(1232)$ resonance and its subsequent decay into $N\pi$), the model also includes background terms required by chiral symmetry. It consists of seven diagrams (see Fig. 1): Direct and crossed $\Delta(1232)$—(first row) and nucleon (second row) pole terms (ΔP, $C\Delta P$, NP, CNP) contact (CT) and pion-pole (PP) contribution (third row) and finally the pion-in-flight (PF) term. It provides a fairly good description of all available data for pion production off the nucleon at intermediate energies, driven by CC and NC and induced by both neutrino and antineutrino [33]. To compute

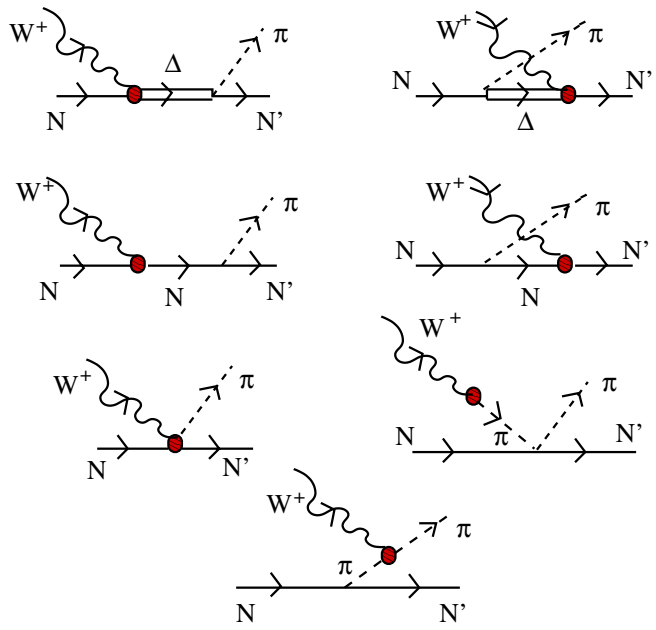

FIG. 1 (color online). Model of Ref. [33] for the $W^+N \to N'\pi$ reaction. The circle in the diagrams stands for the weak transition vertex.

$\mathcal{J}^{\mu}_{N\pi^+}(\vec{r};q,k_\pi)$, we will need to evaluate

$$\frac{1}{2}\sum_r \bar{u}_r(\vec{p}')\Gamma^{\mu}_{i;N\pi^+}u_r(\vec{p}),$$
$$i=\Delta P, C\Delta P, NP, CNP, CT, PP, PF \tag{6}$$

where the u's are Dirac spinors for the nucleons, normalized such that $\bar{u}u=2M$, and the four-vector matrices $\Gamma^{\mu}_{i;N\pi^+}$ can be read from the explicit expressions of the pion production amplitudes $\langle N\pi^+|j^{\mu}_{cc+}(0)|N\rangle=\sum_i \bar{u}(\vec{p}')\Gamma^{\mu}_{i;N\pi^+}u(\vec{p})$ in Eq. (51) of Ref. [33]. Finally, $\vec{p}$ and $\vec{p}'=\vec{p}+\vec{q}-\vec{k}_\pi$ are the initial and final three momenta of the nucleon. Those momenta are not well defined and we approximate the four-momentum of the nucleon N which collides with the W^+ by

$$p^{\mu}=\left(\sqrt{M^2+\frac{1}{4}(\vec{k}_\pi-\vec{q})^2},\frac{\vec{k}_\pi-\vec{q}}{2}\right). \tag{7}$$

Hence we assume that the initial nucleon momentum is $(\vec{k}_\pi-\vec{q})/2$ and the final one is $-(\vec{k}_\pi-\vec{q})/2$, with both nucleons being on-shell. The momentum transfer is equally shared between the initial and final nucleon momenta. This prescription was firstly used in Refs. [54,55] for coherent π^0 photo- and electroproduction, respectively. The approximation is based on the fact that, for Gaussian nuclear wave functions, it leads to an exact treatment of the terms linear in momentum of the elementary amplitude. In Ref. [54] it was shown that this prescription provided similar results as the explicit sum for the nucleon momenta performed in Ref. [57]. More recently it has also been employed in Refs. [58,59] for coherent π^0 photo- and electroproduction and in a recent work on neutrino coherent pion production [31,32]. Setting $\vec{p}=-\vec{p}'=(\vec{k}_\pi-\vec{q})/2$, with energies $p^0=p'^0$ given by Eq. (7), eliminates some nonlocal contributions, and it greatly simplifies the sum over all nucleons, which can be cast in terms of the neutron and proton densities (see Eq. (5)). Furthermore, the sum over helicities in Eq. (6) can be also easily performed for $\vec{p}=-\vec{p}'$ since $u_r(\vec{p}'=-\vec{p})=\gamma^0 u_r(\vec{p})$, so that

$$\frac{1}{2}\sum_r \bar{u}_r(\vec{p}'=-\vec{p})\Gamma^{\mu}_{i;N\pi^+}u_r(\vec{p})=\frac{1}{2}\,\mathrm{Tr}((\not{p}+M)\gamma^0\Gamma^{\mu}_{i;N\pi^+}),$$
$$i=\Delta P, C\Delta P, NP\ldots. \tag{8}$$

Thus finally, we will use

$$\mathcal{J}(\vec{r};q,k_\pi)=\sum_i \mathcal{J}^{\mu}_{i;N\pi^+}(\vec{r};q,k_\pi),$$
$$i=\Delta P, C\Delta P, NP, CNP, CT, PP, PF \tag{9}$$

$$\mathcal{J}^{\mu}_{i;N\pi^+}(\vec{r};q,k_\pi)=\frac{1}{2}\,\mathrm{Tr}((\not{p}+M)\gamma^0\Gamma^{\mu}_{i;N\pi^+})\frac{M}{p^0}, \tag{10}$$

expressions that we shall evaluate numerically. Note that the PF term does not contribute to the process since the trace above is zero in this case. Within this approximation, the averaged $W^+N\to N\pi^+$ amplitude inside the nuclear medium, $\mathcal{J}^{\mu}_{N\pi^+}(\vec{r};q,k_\pi)$, does not depend on $\vec{r}$. Below, we will include further medium corrections to the dominant ΔP mechanism which will induce an explicit $\vec{r}$ dependence.

Given the importance of the Δ-pole contribution and since the Δ properties are strongly modified inside the nuclear medium [60–63], we consider some additional nuclear corrections to this contribution to include the effect of the self-energy of the Δ in the medium $\Sigma_\Delta(\rho(\vec{r}))$. Here we follow the same approach as in Ref. [31], which is based on the findings of Refs. [62–64]. Thus in the Δ-propagator, we make the substitutions $M_\Delta\to M_\Delta+\mathrm{Re}\Sigma_\Delta$ and $\Gamma_\Delta/2\to\Gamma^{\mathrm{Pauli}}_\Delta/2-\mathrm{Im}\Sigma_\Delta$ and take $\Sigma_\Delta(\rho(\vec{r}))$ and $\Gamma^{\mathrm{Pauli}}_\Delta/2$ as explained in Sect. II B of Ref. [31].

So far the formalism has used the bound wave functions of the nucleus, which appear via the proton and neutron densities, and has considered only a plane wave for the pion. Pion distortion effects are important, especially for $|\vec{k}_\pi|<0.5$ GeV [29–32], and are considered here by replacing in Eq. (5)

$$e^{-i\vec{k}_\pi\cdot\vec{r}}\to\tilde{\varphi}^*_{\pi^+}(\vec{r};\vec{k}_\pi) \tag{11}$$

$$\vec{k}_\pi e^{-i\vec{k}_\pi\cdot\vec{r}}\to i\vec{\nabla}\tilde{\varphi}^*_{\pi^+}(\vec{r};\vec{k}_\pi). \tag{12}$$

The pion wave function $\tilde{\varphi}^*_{\pi^+}(\vec{r};\vec{k}_\pi)$ corresponds to an incoming solution of the Klein-Gordon equation,

$$[-\vec{\nabla}^2+m_\pi^2+2E_\pi V_{\mathrm{opt}}(\vec{r})]\tilde{\varphi}^*_{\pi^+}(\vec{r};\vec{k}_\pi)=E^2_\pi\tilde{\varphi}^*_{\pi^+}(\vec{r};\vec{k}_\pi), \tag{13}$$

with $V_{\mathrm{opt}}(\vec{r})$ the optical potential which describes the π^+-nucleus interaction. This potential has been developed microscopically and it is explained in detail in Refs. [63,64]. It contains the ordinary lowest-order optical potential pieces constructed from the s- and p-wave πN amplitudes. In addition second-order terms in both s- and p-waves, responsible for pion absorption, are also considered. Standard corrections, as second-order Pauli rescattering term, angular transform term (ATT), Lorentz-Lorenz effect and long- and short-range nuclear correlations, are also taken into account. This theoretical potential reproduces fairly well the data of pionic atoms (binding energies and strong absorption widths) [63] and low-energy π-nucleus scattering [64]. At low pion energies, it is an improvement over the one used in [31,32], which was based on Δ dominance of the πN interaction. Another possible improvement would be the inclusion of the Coulomb interaction between the outgoing pion and the nucleus. This can be taken into account by means of the

replacement

$$E_\pi \to E_\pi - V_C(\vec{r}) \tag{14}$$

in the right-hand side of Eq. (13), where $V_C(\vec{r})$ is the Coulomb potential created by the nucleus, including finite size and vacuum polarization effects, see [63,64]. We will discuss the effect of this correction in Sec. IV.

The replacement in Eq. (12), which takes into account the fact that the pion three-momentum is only well defined asymptotically when the pion-nucleus potential vanishes, induces some nonlocalities in the amplitudes. To treat these nonlocalities we have adopted the following scheme:

(i) In Eq. (4), we approximate $|\vec{k}_\pi|$, which arises from the phase space integrations, by the modulus of the asymptotic three momentum $(E_\pi^2 - m_\pi^2)^{1/2}$.

(ii) In the ΔP, $C\Delta P$, NP, CNP terms, we note that there exist either a $NN\pi$ or a $N\Delta\pi$ vertex (see Eq. (51) of Ref. [33]), which induces a factor k_π^α in the amplitudes. Indeed, for those terms we could rewrite

$$\mathcal{J}^\mu_{i;N\pi^+}(\vec{r};q,k_\pi) = (k_\pi)_\alpha \hat{\mathcal{J}}^{\mu\alpha}_{i;N\pi^+}(\vec{r};q,k_\pi), \quad i = \Delta P, C\Delta P, NP, CNP. \tag{15}$$

We do not consider any nonlocality in the tensor $\hat{\mathcal{J}}^{\mu\alpha}_{i;N\pi^+}$, and we use the prescription of Eqs. (11) and (12) to account for $\vec{k}_\pi$ in the contraction between k_π^α and $\hat{\mathcal{J}}^{\mu\alpha}_{i;N\pi^+}$ in Eq. (15). This approach to treat the nonlocalities is equivalent to that assumed in Refs. [31,32].

(iii) We do not consider any nonlocality for the CT and PP contributions.

Antineutrinos induce the coherent production of negatively charged pions. To study these processes, we use [33]

$$L^{(\bar{\nu})}_{\mu\sigma} = L^{(\nu)}_{\sigma\mu} \tag{16}$$

$$\mathcal{J}^\mu_{p\pi^-[n\pi^-]}(\vec{r};q,k_\pi) = \mathcal{J}^\mu_{n\pi^+[p\pi^+]}(\vec{r};q,k_\pi) \tag{17}$$

and implement the appropriate changes in the pion-nucleus $V_{\rm opt}$ and V_C potentials to properly account for the distortion of the outgoing π^- [64].

Differences between neutrino and antineutrino induced cross sections are proportional to the interferences among the axial and vector current contributions. Since the latter ones are suppressed by the nuclear form factor, as we discussed after Eq. (5), we expect roughly similar neutrino and antineutrino cross sections. This will also be the case for the NC driven processes studied in the next section.

III. NC NEUTRINO AND ANTINEUTRINO INDUCED REACTIONS

To extend the above formulae to the case of NC π^0 coherent production,

$$\nu_l(k) + A_Z|_{gs}(p_a) \to \nu_l(k') + A_Z|_{gs}(p'_a) + \pi^0(k_\pi) \tag{18}$$

we have,

$$\frac{d^5\sigma_{\nu\nu}}{d\Omega(\hat{k}')dE'd\Omega(\hat{k}_\pi)} = \frac{|\vec{k}'|}{|\vec{k}|}\frac{G^2}{16\pi^2}L^{(\nu)}_{\mu\sigma}W^{\mu\sigma}_{{\rm NC}\pi^0} \tag{19}$$

$$W^{\mu\sigma}_{{\rm NC}\pi^0} = \frac{|\vec{k}_\pi|}{64\pi^3M^2}\mathcal{A}^\mu_{\pi^0}(q,k_\pi)(\mathcal{A}^\sigma_{\pi^0}(q,k_\pi))^* \tag{20}$$

$$A^\mu_{\pi^0}(q,k_\pi) = \int d^3\vec{r}e^{i\vec{q}\cdot\vec{r}}\{\rho_p(\vec{r})[\mathcal{J}^\mu_{p\pi^0}(\vec{r};q,k_\pi)] + \rho_n(\vec{r})[\mathcal{J}^\mu_{n\pi^0}(\vec{r};q,k_\pi)]\}\tilde{\varphi}^*_{\pi^0}(\vec{r};\vec{k}_\pi) \tag{21}$$

with $\vec{k}'$ and $E' = |\vec{k}'|$ the LAB outgoing neutrino momentum and energy. The leptonic tensor is given in Eq. (3) and it is now orthogonal to $q^\mu = (k-k')^\mu$ for massless neutrinos, i.e., $L^{(\nu)}_{\mu\sigma}q^\mu = L^{(\nu)}_{\mu\sigma}q^\sigma = 0$.

Both lepton and hadron tensors are independent of the neutrino lepton family, and therefore the cross section for the reaction of Eq. (18) is the same for electron, muon or tau incident neutrinos. Furthermore, the hadron tensor is the same for neutrino and antineutrino induced reactions, and thus to study antineutrino reactions we just have to change the sign of the antisymmetric part of the leptonic tensor (see Eq. (16)).

To evaluate the hadronic tensor, we use the model for the NC pion production off the nucleon derived in Ref. [33] and thus we have

$$\mathcal{J}(\vec{r};q,k_\pi) = \sum_i \mathcal{J}^\mu_{i;N\pi^0}(\vec{r};q,k_\pi), \quad i = \Delta P, C\Delta P, NP, CNP, CT, PP, PF \tag{22}$$

$$\mathcal{J}^\mu_{i;N\pi^0}(\vec{r};q,k_\pi) = \frac{1}{2}\,{\rm Tr}((\not{p}+M)\gamma^0\Gamma^\mu_{i;N\pi^0})\frac{M}{p^0}, \tag{23}$$

with the same prescription for the nucleon momentum as in the CC case. Within this model the PP, PF and CT diagrams do not contribute to the NC π^0 production off the nucleon. The ΔP and $C\Delta P$ terms provide equal $Z^0p \to p\pi^0$ and $Z^0n \to n\pi^0$ amplitudes, with $\Gamma^\mu_{\Delta P;N\pi^0}$ and $\Gamma^\mu_{C\Delta P;N\pi^0}$ obtained from $\Gamma^\mu_{\Delta P;p\pi^+}$ and $\Gamma^\mu_{C\Delta P;p\pi^+}$ multiplying these latter matrices by the overall factors $2\sqrt{2}/(3\cos\theta_C)$ and $2\sqrt{2}/\cos\theta_C$, respectively, and multiplying the vector form factors by $(1-2\sin^2\theta_W)$, being θ_C the Cabibbo angle and θ_W the Weinberg angle. Direct and crossed nucleon pole terms lead to

$$\Gamma^{\mu}_{NP;N\pi^0} = -iD^{NP}\frac{g_A}{2f_\pi}\not{k}_\pi\gamma_5\frac{\not{p}+\not{q}+M}{(p+q)^2-M^2+i\epsilon} \times (V^{\mu}_{Z;N}(q)-A^{\mu}_{Z;N}(q)),$$
$$D^{NP} = \begin{pmatrix} 1 & p\pi^0 \\ -1 & n\pi^0 \end{pmatrix} \quad (24)$$

$$\Gamma^{\mu}_{CNP;N\pi^0} = -iD^{CNP}\frac{g_A}{2f_\pi}(V^{\mu}_{Z;N}(q)-A^{\mu}_{Z;N}(q)) \times \frac{\not{p}-\not{k}_\pi+M}{(p-k_\pi)^2-M^2+i\epsilon}\not{k}_\pi\gamma_5,$$
$$D^{CNP} = \begin{pmatrix} 1 & p\pi^0 \\ -1 & n\pi^0 \end{pmatrix} \quad (25)$$

with $f_\pi \simeq 93$ MeV the pion weak decay constant, $g_A = 1.26$ the axial nucleon coupling, and

$$V^{\alpha}_{Z;N} = 2\times\left[F_1^Z(q^2)\gamma^\alpha + i\frac{\mu_Z F_2^Z(q^2)}{2M}\sigma^{\alpha\nu}q_\nu\right]_N, \quad (26)$$

$$A^{\alpha}_{Z;N} = \left[G_A^Z(q^2)\gamma^\alpha\gamma_5 + \left((G_A^Z(q^2)+G_A^s(q^2))\frac{\not{q}}{m_\pi^2-q^2} + G_P^s(q^2)\right)q^\alpha\gamma_5\right]_N. \quad (27)$$

The pseudoscalar part of the axial current, which is proportional to q^μ, does not contribute to the differential cross section for massless neutrinos. Besides the Z^0NN form factors are given by [65]:

$$(F_1^Z)^{p,n} = \pm F_1^V - 2\sin^2\theta_W F_1^{p,n} - \frac{1}{2}F_1^s \quad (28)$$

$$(\mu_Z F_2^Z)^{p,n} = \pm\mu_V F_2^V - 2\sin^2\theta_W\mu_{p,n}F_2^{p,n} - \frac{1}{2}\mu_s F_2^s \quad (29)$$

$$(G_A^Z)^{p,n} = \pm G_A - G_A^s. \quad (30)$$

For isoscalar nuclei, the direct and crossed nucleon pole terms do not contribute because the existing cancellation between neutron and proton contributions, and we have total dominance of the Δ mechanisms. If we neglect the vector current contributions,[2] finite lepton mass effects and approximating $\cos\theta_C \approx 1$, we find that the CC coherent pion production cross section is twice the NC one, as deduced from the relevant isospin factors and the factor of 4 of difference between Eqs. (2) and (19), for CC and NC driven processes, respectively.[3] For nonsymmetric nuclei, as long as the Δ dominance holds, we will reach the same conclusion. Nevertheless, we reiterate here that for low and intermediate muon neutrino energies ($\leq$ 1.5–2 GeV), one should expect sizable corrections (25% at 1.3 GeV, and greater at smaller energies) to the approximate relation $\sigma_{CC} \approx 2\sigma_{NC}$ due to the finite muon mass [12].

To evaluate pion distortion effects we compute the π^0—wave function by using the appropriate pion-nucleus optical potential [64] and setting $V_C = 0$. Nonlocalities in the amplitudes are treated as in the CC case.

IV. RESULTS

We shall always use the full model of Ref. [33] where the dominant C_5^A nucleon-to-Δ axial form factor was fitted to data resulting in $C_5^A(0) = 0.867$ and $M_{A\Delta} = 0.985$ GeV. Note that the Goldberger-Treiman relation, traditionally assumed in the literature, implies a larger value of $C_5^A(0) \sim 1.2$. We will come back to this point below.

First, we compile in Table I the input charge densities, taken from Ref. [66], used in this work. For each nucleus we take the neutron matter density approximately equal (but normalized to the number of neutrons) to the charge density, though we consider small changes, inspired by Hartree-Fock calculations with the density-matrix expansion [67] and corroborated by pionic atom data [68]. However, charge (neutron) matter densities do not correspond to proton (neutron) pointlike densities because of the finite size of the nucleon. This is taken into account by following the procedure outlined in Sec. 2 of Ref. [68] (see Eqs. (12)–(14) of this reference).

A. General results

First, in Fig. 2 we show the pion momentum distribution (LAB) for CC and NC coherent pion production induced by ν_μ and $\bar{\nu}_\mu$ on a ^{16}O (CC case) and ^{12}C (NC case) targets. In the upper panels we show the CC case for a ν_μ, $\bar{\nu}_\mu$ beam energy of 600 MeV, which is in the expected peak energy region of the future T2K experiment. In the lower two panels we show NC results for a ν, $\bar{\nu}$ beam energy of 850 MeV. In all panels, the short-dashed line corresponds to our results in plane wave impulse approxi-

TABLE I. Charge (r_p, a) and neutron matter (r_n, a) density parameters for different nuclei as given in Ref. [66]. For carbon and oxygen we use a modified harmonic oscillator density, $\rho(r) = \rho_0(1+a(r/r_N)^2)\exp(-(r/r_N)^2)$, while for lead, we use a two-parameter Fermi distribution, $\rho(r) = \rho_0/(1+\exp((r-r_N)/a))$.

Nucleus	r_p [fm]	r_n [fm]	a
^{12}C	1.692	1.692	1.082
^{16}O	1.833	1.833	1.544
^{208}Pb	6.624	6.890	0.549 fm

[2]They will be suppressed by the nuclear form factor (see discussion after Eq. (5)).

[3]For the case of isoscalar nuclei, the approximate relation $\sigma_{CC} \approx 2\sigma_{NC}$ is far more general and it can be directly deduced from PCAC and isospin invariance.

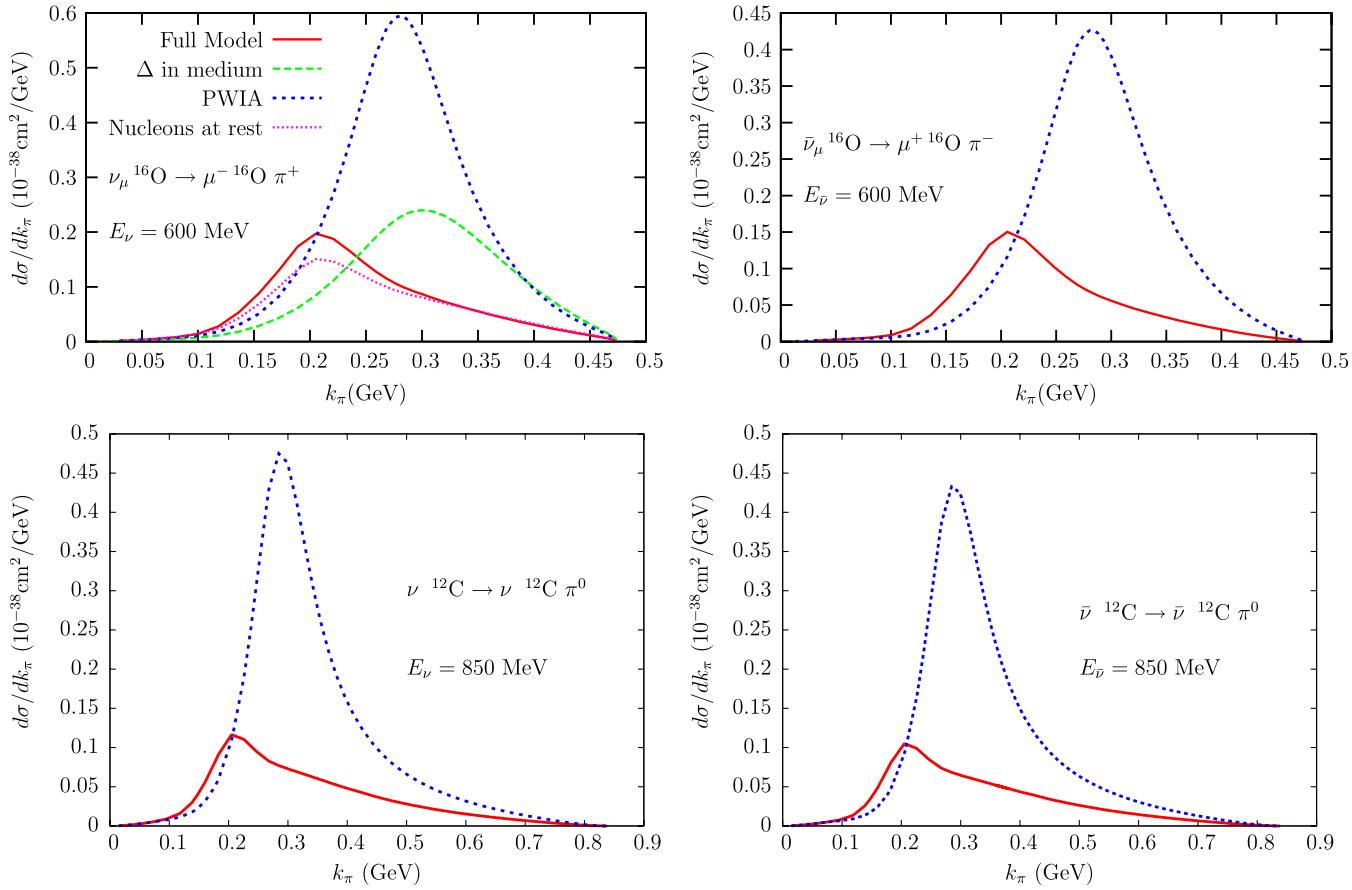

FIG. 2 (color online). Pion momentum differential cross section in the LAB frame for different coherent pion production reactions. Short-dashed line (in blue) has been calculated using planes waves for the outgoing pion and without including any in-medium correction for the Δ. Results with Δ nuclear medium effects are shown in the upper-left panel by the long-dashed line (in green). Our full model calculation, including medium effects on the Δ and the distortion of the outgoing pion wave function, is shown by the solid line (in red). Finally, the effect of putting the nucleons at rest is shown in the upper-left panel by the dotted line (in magenta).

mation (PWIA), in which we use a plane wave for the outgoing pion and neglect medium effects on the dominant Δ contribution. Medium effects introduced through the Δ self-energy play a very important role largely reducing the PWIA results. This is shown by the long-dashed line in the upper-left panel. When the pion distortion is also taken into account (via the substitutions of Eqs. (11) and (12)) the cross section is further reduced, and the peak is shifted towards lower energies reflecting the strong absorption and the higher probability of a quasielastic collision of the outgoing pion by the nucleus in the Δ kinematical region. The total cross section reduction is around 60% for a beam energy of 600 MeV. Our full model results thus obtained are shown by the solid line. Medium and pion distortion effects in coherent pion production were already evaluated in Refs. [31,32]. However in these works the motion of the nucleon was neglected. This is to say, though the authors of these references also use the prescription $\vec{p} = -\vec{p}\,' = (\vec{k}_\pi - \vec{q})/2$ to compute the elementary $W^\pm(Z^0)N \to \pi N'$ amplitude, however the nucleon momenta in the Dirac's spinors appearing in Eq. (8) are neglected. The effect of putting the nucleons at rest can be clearly seen in the dotted line of the upper-left panel and results in a ∼15% decrease of the total cross section. Results obtained for the antineutrino CC induced reaction are shown in the upper-right panel. The cross section is some 30% smaller than in the neutrino case due to the sign change in the axial part of the lepton tensor which results in a different vector-axial interference. Similar effects are seen for NC reactions shown in the lower panels of Fig. 2. In this case the antineutrino cross section is reduced by just 10% with respect to the neutrino one.

In Fig. 3 we show the effect of Coulomb distortion on the outgoing charged pion. One can see the expected shift in the peak towards higher (lower) energies of the positive (negative) pion distribution when the Coulomb distortion is taken into account. The net effect in the total cross section is nevertheless small, amounting to a 5% change for beam energies in the 500 MeV region. For higher energies the effect is expected to be less important.

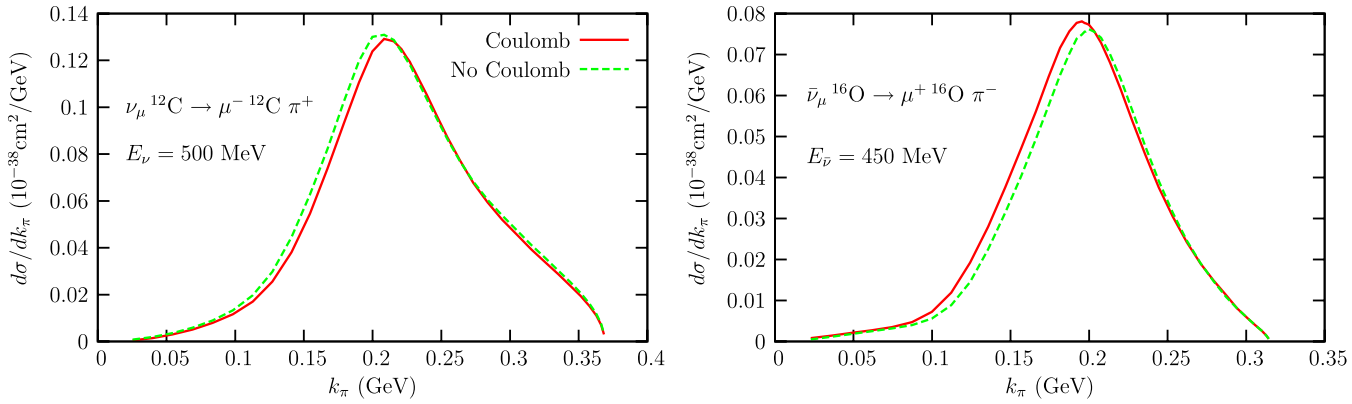

FIG. 3 (color online). Coulomb distortion effects on the pion momentum differential LAB cross section for CC coherent pion reactions induced by ν_μ, $\bar{\nu}_\mu$.

We now study, for CC reactions, the effect of including the background terms on top of the dominant direct (ΔP) and crossed ($C\Delta P$) Δ pole contributions. As mentioned before, the PF term does not contribute to the coherent cross section. Besides, the direct (NP) and crossed (CNP) nucleon pole term contributions partially cancel each other, while the chiral background terms CT, PP vanish for isospin symmetric nuclei due to an exact cancellation between proton and neutron contributions. This latter cancellation is partial for asymmetric nuclei. In the left panel of Fig. 4 we show the results for ^{12}C. As seen in the figure the effect of the background terms, both in the PWIA and in the full calculation (including medium effects and pion distortion), is very small, thus corroborating the findings of Ref. [32]. In the right panel of the figure we show full calculation results for ^{208}Pb , which is the most asymmetric nucleus with possible experimental interest. In this latter case the inclusion of the background terms reduces the cross section in an appreciable way. We find similar conclusions for NC driven processes.

This predominant role played by the Δ mechanism, in conjunction with the findings of Ref. [33] and the fact that the coherent pion production reaction in nuclei is mostly driven by the axial part of the interaction, allows us to conclude that most of the previous theoretical studies [9,12,27,30,31] of the pion coherent channel might be overestimating the cross section roughly by a factor of 2. This can be easily understood as follows. Background terms turned out to be very important at the nucleon level and because of them, the flux-averaged $\nu_\mu p \to \mu^- p \pi^+$ ANL q^2-differential cross section [47,48] is described with an axial form factor $C_5^A(0)$ of around 0.9 [33], significantly smaller than the traditionally used value of about 1.2, deduced from the Goldberger-Treiman relation. This reduction of the contribution of the Δ pole mechanism in the weak pion production off the nucleon is compensated by the nonresonant terms. However, when one studies the neutrino coherent pion production in isoscalar nuclei we find a negligible contribution of the nonresonant terms, and thus the cross section is determined by the axial part of the Δ mechanism of which C_5^A gives the largest contribution. Thus, we predict cross sections around a factor of $(1.2/0.9)^2 \sim 2$ smaller than those approaches which assume the Goldberger-

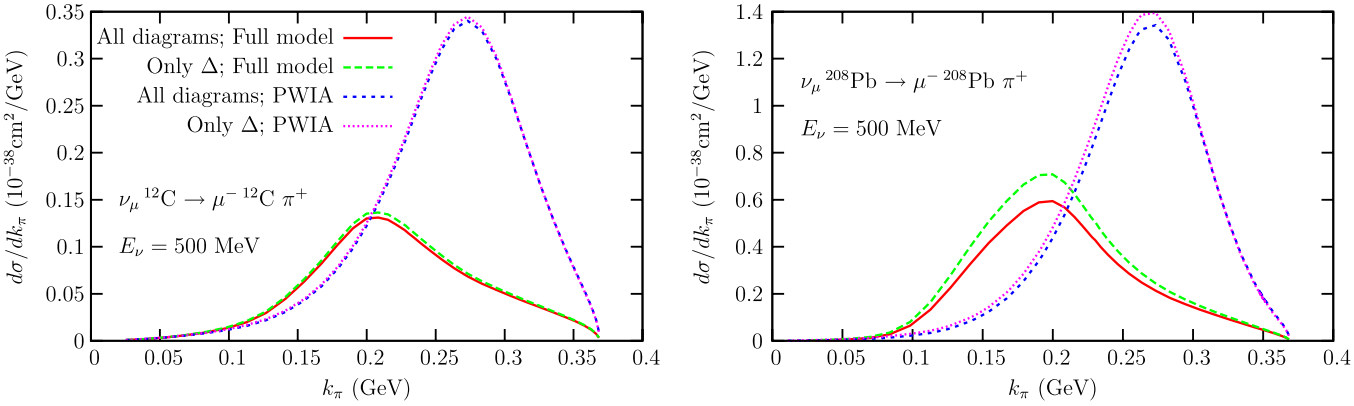

FIG. 4 (color online). Pion momentum differential LAB cross section, calculated with and without background terms, for CC coherent pion production induced by a 500 MeV ν_μ beam. The curves labeled as "Only Δ" stand for results obtained from the ΔP and $C\Delta P$ mechanisms. Left panel: results for a ^{12}C target and PWIA and full calculations; Right panel: results for a ^{208}Pb target.

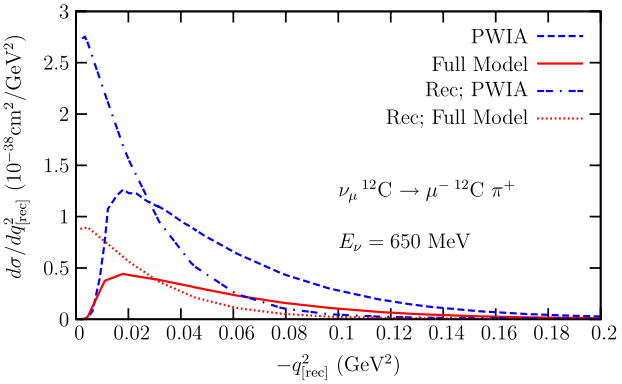

FIG. 5 (color online). Differential $d\sigma/dq^2$ and LAB $d\sigma/dq^2_{\mathrm{rec}}$ distributions from carbon target, calculated both within the PWIA and using our full model. In the x-axis, $-q^2$ or LAB $-q^2_{\mathrm{rec}}$ values are displayed, depending on the curve.

Treiman relation.[4] This fact was first pointed out by the authors of Ref. [32], who used for the very first time the background terms derived in Ref. [33] for the elementary reaction. However, we improve here the results of this reference by properly taking into account the motion of the nucleons, as discussed above, and correcting for some numerical inaccuracies [52] (of the order of 20% in the total cross section, and larger at the peak of the $d\sigma/dk_\pi$ differential distribution) that affected the calculations of this reference and those of a previous work by the same authors [31].

Next we pay attention to the q^2 differential cross section, and in Fig. 5 we show this distribution for ν_μ CC driven processes in the energy region of the future T2K experiment. There, we also show $d\sigma/dq^2_{\mathrm{rec}}$, where q^2_{rec} is calculated, under the assumption of a Quasi-Elastic (QE) neutrino–nucleon interaction, from the measured outgoing lepton energy and scattering angle in the LAB frame,

$$q^2_{\mathrm{rec}} = -2Mq^0_{\mathrm{rec}} = -2M(E^{\mathrm{rec}}_\nu - E') \tag{31}$$

$$E^{\mathrm{rec}}_\nu = \frac{ME' - m_l^2/2}{M - E' + |\vec{k}'|\cos\theta'}. \tag{32}$$

The q^2_{rec} distribution as compared with the q^2 one is clearly shifted to lower absolute values and peaks roughly at 0. This fact might be used to reduce the QE background by requiring that coherent events should have a reconstructed q^2_{rec} value smaller than some appropriate cut, as was done in the K2K analysis carried out in Ref. [11].

[4]A word of caution is required here. There exists some degree of inconsistency among the ANL [47,48] and BNL [69] measurements of the integrated $\nu_\mu p \to \mu^- p\pi^+$ cross section, the latter being larger than the former one. The model of Ref. [33], including nonresonant background terms, with $C_5^A(0) = 1.2$ (consistent with the off diagonal Goldberger-Treiman relation) would lead to a better description of the BNL data than if the lower vale of around 0.9 is used. Thus, if one favors BNL data one could still use a high value of $C_5^A(0) = 1.2$, which would lead to larger coherent pion production cross sections.

We turn now to angular distributions of the final pion and muon in ν_μ induced CC reactions. In Fig. 6 we show the pion angular LAB distribution with respect to the incoming neutrino direction. As expected, and due to the nucleus form factor, the reaction is very forward peaked. Inclusion of medium effects on the Δ propagator and the final pion distortion largely reduce the cross section. The angular distribution profile keeps its forward peaked behavior, although less pronounced once the pion distortion is included. This can be seen on the right panel where the angular distributions are all equally normalized to one. Such a behavior can be understood by taking into account that the pion wave function $\tilde{\varphi}^*_\pi(\vec{r};\vec{k}_\pi)$ does not have well-defined momentum, in contrast with the plane wave $e^{-i\vec{k}_\pi\cdot\vec{r}}$. Putting the nucleons at rest has some effect on the cross section but hardly affects the angular distribution profile. The situation is very similar for the muon angular distribution, shown in Fig. 7 for CC coherent pion production by a 0.65 GeV energy ν_μ beam on a ^{12}C target. In this case the angular distribution profile is completely unaffected by the nuclear effects on the Δ and the pion distortion.

B. The Rein-Sehgal model and the NC MiniBooNE $E_\pi(1 - \cos\theta_\pi)$ distribution

We have also examined the NC differential cross section with respect to the variable $E_\pi(1 - \cos\theta_\pi)$, proposed by the MiniBooNE Collaboration in its recent analysis of coherent π^0 production of Ref. [18]. Pion variables are referred to the LAB frame. Results are shown in the left top panel of Fig. 8 for a neutrino beam energy of 800 MeV (close to the ν_μ energy peak of the MiniBooNE experiment) on carbon. Our differential cross section is appreciably narrower than that displayed in Fig. 3b of Ref. [18].[5] Indeed, our distribution at $E_\pi(1 - \cos\theta_\pi) = 0.1$ GeV has already fallen off by a factor of 18, while the MiniBooNE distribution has fallen off by less than a factor of 4 at 0.1 GeV, and even at 0.2 GeV the reduction factor is still smaller than 15. We find it hard to understand this discrepancy. Since the excitation of $\Delta(1232)$-resonance mechanism is dominant, we expect the outgoing pion to have a total energy of around 0.25–0.35 GeV (see for instance left bottom panel of Fig. 2). On the other hand, we find that the cross section is almost negligible for $\cos\theta_\pi > 0.7$, as can

[5]Note however, that the $E_\pi(1 - \cos\theta_\pi)$ distributions shown in Ref. [18] are not proper differential cross sections. This is because they have not been corrected for acceptance or cut efficiencies and are plotted for reconstructed kinematic quantities. So they include the effects of the selection criterion (the efficiency of which can vary as a function of $E_\pi(1 - \cos\theta_\pi)$), as well as reconstruction effects in the MiniBooNE detector. Currently, the MiniBooNE Collaboration is working to have all of the effects of the detector, event reconstruction, and selection removed. The new results will follow in an upcoming paper, where actual differential cross sections will be available [70].

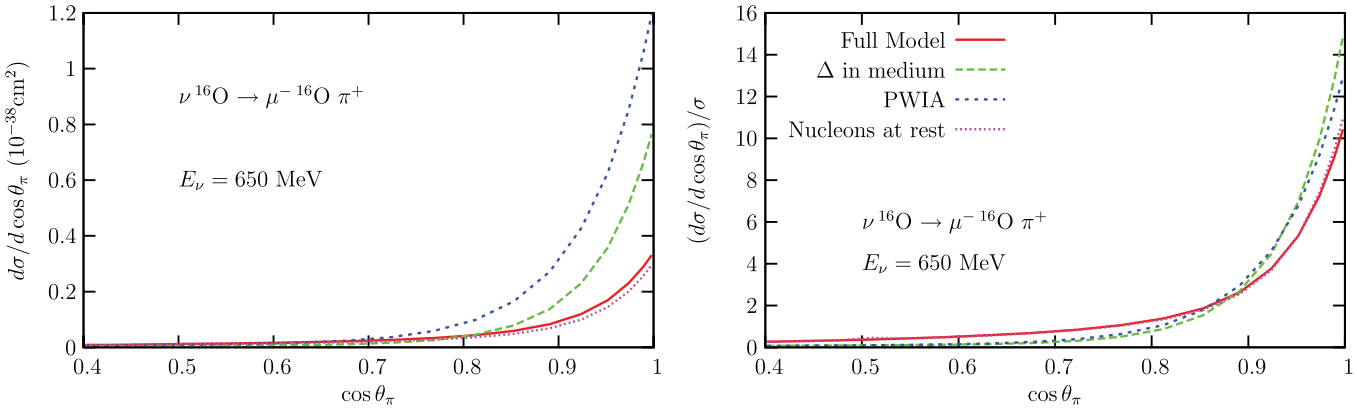

FIG. 6 (color online). Pion angular differential cross section for CC coherent pion production by a ν_μ beam of 650 MeV energy on a ^{16}O target. Left panel: absolute differential cross section; Right panel: differential cross sections normalized to one. The θ_π angle is referred to the incoming neutrino direction in the LAB frame.

be inferred from the pion angular LAB differential cross section displayed in the right top panel of Fig. 8. Thus, we easily understand why we find that the $E_\pi(1-\cos\theta_\pi)$ distribution becomes quite small above 0.1 GeV. To have non-negligible signals in the $E_\pi(1-\cos\theta_\pi) = 0.1$–$0.2$ GeV region would require, approximately, values of $\cos\theta_\pi$ in the interval $2/3 - 1/3$, which would translate into values of θ_π in the range 50°–70°. Since $\vec{q}$ is strongly aligned to the incoming neutrino direction, such high pion angles look hardly compatible with the forward character of the coherent reaction, which is just imposed by the nucleus form factor (Fourier transform of the nuclear density for momentum $\vec{q} - \vec{k}_\pi$) and the $\vec{q}\cdot\vec{k}_\pi$ dependence of the amplitudes (dominated by the axial contribution).

The strong disagreement between our prediction and the MiniBooNE histogram in the region below $E_\pi(1-\cos\theta_\pi) < 0.1$ GeV is even more worrisome, because there the cross sections are much larger. We are aware that within the ν_μ MiniBooNE flux, there exist neutrino energy components higher and smaller than the 800 MeV considered in the top panels of Fig. 8. In the left bottom panel of Fig. 8, we show the $E_\pi(1-\cos\theta_\pi)$ differential cross section for three more neutrino energies (300, 550 and 1300 MeV), in addition to that of 800 MeV considered in the top panels. In all cases, we find very small signals for $E_\pi(1-\cos\theta_\pi)$ above 0.05 GeV. Also in this panel, we show our $E_\pi(1-\cos\theta_\pi)$ differential cross section convoluted with the ν_μ MiniBooNE flux (solid line), and we certainly find a distribution definitely narrower than that published in Ref. [18].

Since the MiniBooNE analysis relies on the Rein-Sehgal model for coherent π^0 production [9], the strong shape difference should be understood in terms of the differences between our model and that of Ref. [9].

1. The t-dependence of the Rein-Sehgal model

Rein and Sehgal made use of the Adler's PCAC formula [10] and approximated (both for neutrino or antineutrino-

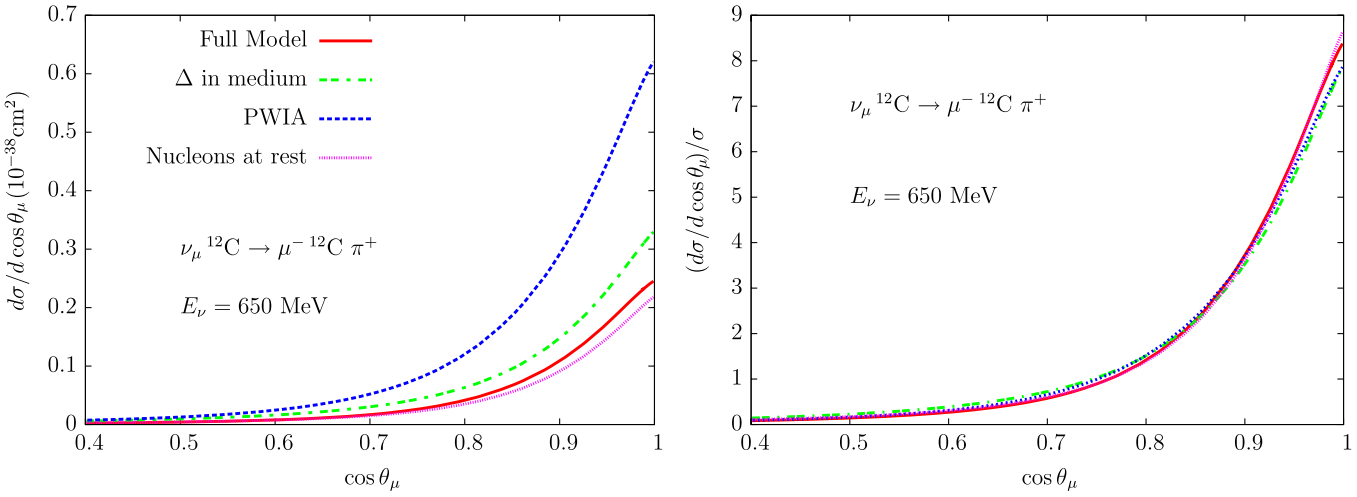

FIG. 7 (color online). Muon angular differential cross section for CC coherent pion production induced by a 650 MeV energy ν_μ beam on a ^{12}C target. Left panel: absolute differential cross section; Right panel: differential cross sections normalized to one. The θ_μ angle is referred to the incoming neutrino direction in the LAB frame.

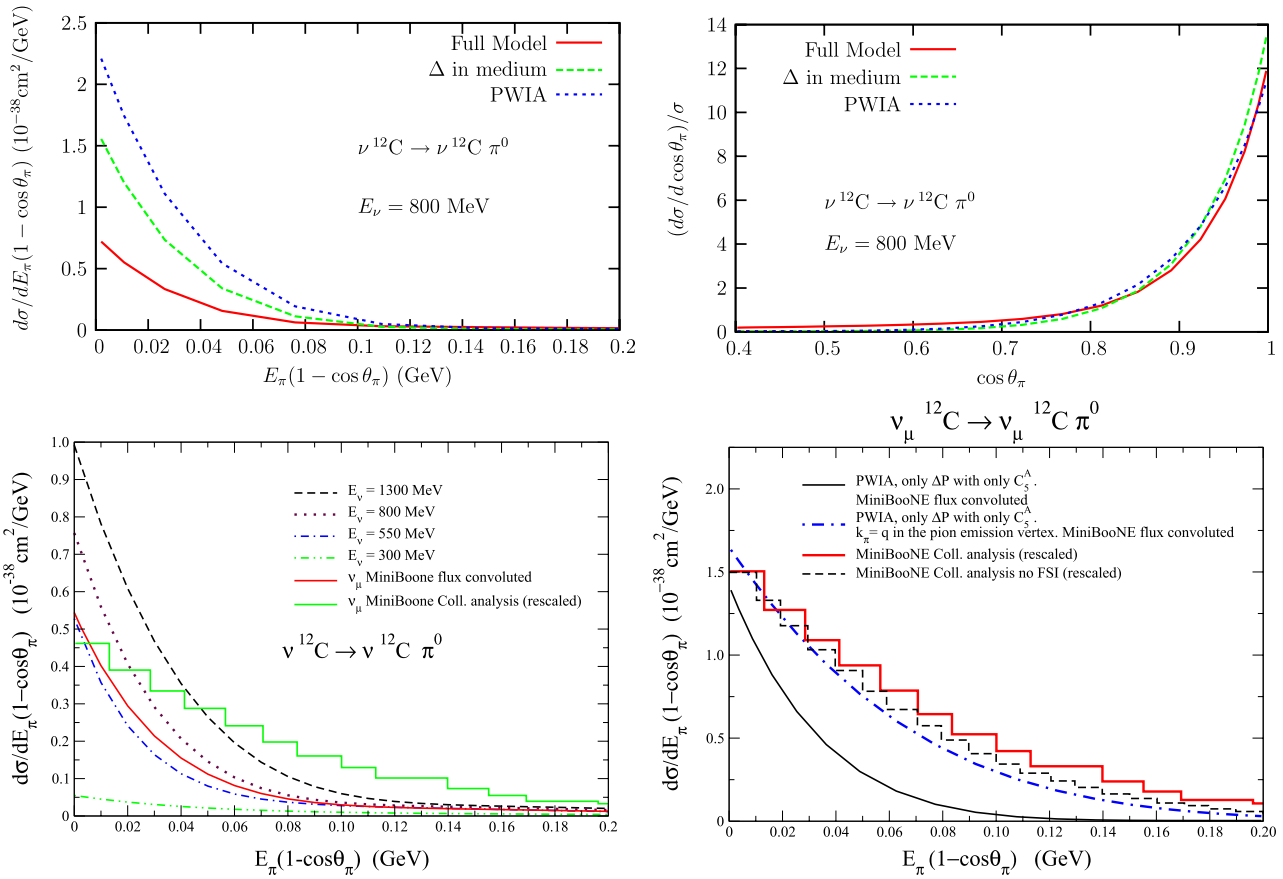

FIG. 8 (color online). Laboratory $E_\pi(1-\cos\theta_\pi)$ and $\cos\theta_\pi$ distributions for the $\nu^{12}\mathrm{C} \to \nu^{12}\mathrm{C}\pi^0$ reaction, at MiniBooNE energies. Different models are considered in the upper panels, while our full model is always used in the left bottom one, where we also show the $E_\pi(1-\cos\theta_\pi)$ distribution convoluted with the ν_μ MiniBooNE flux (solid line). Details of the convolution are explained in the text (see Eq. (36) and Table II). In the right bottom panel, we show results from the C_5^A axial contribution of the ΔP mechanism, neglecting pion distortion and Δ in-medium effects (see the text for the explanation of the two curves). In both bottom panels, we display the MiniBooNE published histogram (solid), conveniently scaled down, taken from the right panel of Fig. 3 in Ref. [18]. Finally, in the right bottom panel, we also show MiniBooNE results (dashed histogram) obtained by turning off the NUANCE FSI of the outgoing pion (G. Zeller private communication).

induced processes) the coherent π^0 production differential cross section by

$$\left(\frac{d\sigma_{\nu\nu}}{dxdyd|t|}\right)_{q^2=0} = \frac{G^2 M E_\nu}{\pi^2} f_\pi^2 (1-y)\Big(|F_{\mathcal{A}}(t)|^2 F_{\mathrm{abs}} \times \frac{d\sigma(\pi^0 N \to \pi^0 N)}{d|t|}\Big|_{q^0=E_\pi, t=0}\Big) \quad (33)$$

with $x = -q^2/2Mq^0$, $y = q^0/E_\nu$, and $t = (q-k_\pi)^2 = -(\vec{q}-\vec{k}_\pi)^2$. Besides, the nuclear form factor is calculated as $F_{\mathcal{A}}(t) = \int d^3\vec{r} e^{i(\vec{q}-\vec{k}_\pi)\cdot\vec{r}}\{\rho_p(\vec{r}) + \rho_n(\vec{r})\}$, and finally F_{abs} is a t-independent attenuation factor.[6] The above expression was deduced in the so-called parallel configuration, for which the k_μ and k'_μ four momenta are proportional (therefore $q^2 = 0$) and $\cos\theta_{qk_\pi}$ (angle formed by $\vec{k}_\pi$ and $\vec{q}$) and $|\vec{k}_\pi|/|\vec{q}|$ are approximated to one everywhere except in the nuclear form factor. It was continued to nonzero q^2 values by including a propagator term of the form $(1 - q^2/m_A^2)^{-2}$, with $m_A \approx 1$ GeV. The model should work well close to this parallel kinematics, and constitutes a good approximation at the high neutrino energies, above 2 GeV, explored in the original work of Ref. [9]. However, the approximations in which this model is based become less justified as the neutrino energy decreases. For the energies relevant in the MiniBooNE and T2K experiments, nonparallel configurations turn out to be more important, and the Rein-Sehgal model predictions are less reliable.

Actually, we see from Eq. (33) that the Rein-Sehgal differential cross section depends on $\cos\theta_\pi$ or t only through the nuclear form factor, and any further $\cos\theta_\pi$ and/or t behavior induced by the dependence of the amplitudes on k_π is totally neglected. However, it is reason-

[6] In the original work of Ref. [9], it is stated that F_{abs} takes into account effects of pion absorption in the nucleus. As defined in Ref. [9], F_{abs} only removes from the flux pions that undergo inelastic collisions but, as explained below, no true absorption is actually included.

able to expect that these additional angular dependences might play a role when the pion emission is not completely forward. To illustrate this point, we have rederived Eq. (33) from our model. We have considered the dominant C_5^A axial contribution of the ΔP mechanism and made use, in this case, of the Goldberger-Treiman relation to express $C_5^A(0)$ in terms of the $\pi N\Delta$ coupling, f^*, and the pion decay constant $f_\pi[C_5^A(0) = \sqrt{\frac{2}{3}}\frac{f_\pi}{m_\pi}f^*]$. Besides, we have considered neither the in-medium Δ-self-energy, nor the pion distortion effects. On the other hand, we have used the $N\Delta\pi$ Lagrangian[7]

$$\mathcal{L}_{\pi N\Delta} = \frac{f^*}{m_\pi}\bar{\Psi}_\mu \vec{T}^\dagger(\partial^\mu\vec{\phi})\Psi + \text{H.c.} \tag{34}$$

to compute $d\sigma(\pi^0 N \to \pi^0 N)/d|t|$. To further simplify, we have worked in the nonrelativistic limit for the baryons. Apart from F_{abs}, we reproduce Eq. (33), but with an extra $(\cos\theta_{qk_\pi})^2$ factor in the right-hand side of the equation, which for the case of parallel kinematics is equivalent to $(\cos\theta_\pi)^2$. At high neutrino energies, the pion is emitted strongly forward, and thus it is consistent to approximate this factor by one, as it was done in the original work of Ref. [9] to obtain Eq. (33). For MiniBooNE neutrino energies, relatively large θ_π angles are allowed, especially for low pion momenta ($|\vec{k}_\pi| < 0.2$ GeV) [71], and this factor $(\cos\theta_\pi)^2$ could make the $E_\pi(1-\cos\theta_\pi)$ distribution significantly narrower than that predicted by the Rein-Sehgal model. For a fixed value of $E_\pi(1-\cos\theta_\pi)$, the effect becomes more important as the pion energy decreases. For instance, if we fix $E_\pi(1-\cos\theta_\pi) = 0.05$ GeV, we find that $(\cos\theta_\pi)^2 \approx 1/2$ or $3/4$, for an averaged pion energy of 0.17 or 0.375 GeV, respectively. As it was shown in the talk of J. Link at Nuint07 [71], in the Rein-Sehgal model, low-energy pions ($|\vec{k}_\pi| < 0.5$ GeV) produce wider $E_\pi(1-\cos\theta_\pi)$ shapes than those of higher energies ($|\vec{k}_\pi| > 0.5$ GeV), and thus we expect this type of correction to be important. In addition, there also exist corrections that vanish in the $q^2 \to 0$ (or equivalently $|\vec{q}|/q^0 \to 1$) and/or $|\vec{k}_\pi|/|\vec{q}| \to 1$ (also implied by the $t = 0$ approximation in the amplitudes) limits.

Another way to see the limitations of the Rein-Sehgal model is the following. As mentioned, this model assumes no further dependence on t than that encoded in the nuclear form factor. Since $t = 0$ implies $q = k_\pi$, we have replaced k_π^α in Eq. (15) by q^α. That is to say, we replace k_π by q in the pion emission vertex.[8] To better compare with the Rein-Sehgal predictions, we have again just considered the dominant C_5^A axial contribution of the ΔP mechanism, without considering pion distortion and Δ in-medium effects. ν_μ MiniBooNE flux convoluted results are displayed in the right bottom panel of Fig. 8. We see that the new $E_\pi(1-\cos\theta_\pi)$ distribution is significantly wider than that obtained without implementing this replacement, and that it reasonably describes the MiniBooNE published distribution (solid histogram in the plot). The agreement is much better, when we compare with some preliminary MiniBooNE results (dashed histogram) obtained with a different treatment of the outgoing pion Final State Interaction (FSI), as we will explain in the next subsubsection.[9] Without giving a special meaning to this agreement, this simple calculation serves the purpose of illustrating the uncertainties associated with the $t = 0$ approximation at low energies, for which the nuclear form factor still allows some deviations from the completely forward scattering.

We conclude that the Rein-Sehgal pion coherent production model for MiniBooNE and T2K experiments is not as reliable as for the case of neutrino energies above 2 GeV. We expect sizable corrections to the predictions of this model, both for differential distributions and for integrated cross sections. Our model provides an $E_\pi(1-\cos\theta_\pi)$ distribution much more peaked around zero, and thus it might improve the description of the first bin value in Fig. 3b of Ref. [18]. Moreover, the drastic change in the $E_\pi(1-\cos\theta_\pi)$ distribution shape might produce some mismatch between the absolute normalization of the background, coherent and incoherent yields in the MiniBooNE analysis. On the other hand, and besides the issue of the used value[10] for $C_5^A(0)$, the Rein-Sehgal model, adopted by the MiniBooNE Collaboration in Ref. [18], overestimates by a large factor the coherent integrated cross section for MiniBooNE energies. This is due first to the $t = 0$ approximation in the amplitudes assumed in this model that produces a too wide $E_\pi(1-\cos\theta_\pi)$ distribution, which leads to cross sections larger by about a factor of 2 than those obtained when the t-dependence is properly taken into account (see for instance the different areas below the solid and dashed-dotted curves in the right bottom panel of Fig. 8). Second, because all sorts of in-nuclear-medium effects, like pion absorption or modification of the elementary $\pi N \to \pi N$ cross section[11] inside of the nucleus, which

[7]Here, $\vec{\phi}$ is the pion field, Ψ_μ is a Rarita Schwinger $J^\pi = 3/2^+$ field, and $\vec{T}^\dagger$ is the isospin transition operator (vector under isospin rotations and its Wigner-Eckart irreducible matrix element is taken to be one) from isospin 1/2 to 3/2.

[8]If we were to repeat with this replacement the derivation of Eq. (33) as explained above, we will recover it exactly (apart from F_{abs}), and the correction factor $(\cos\theta_{qk_\pi})^2$ would not appear.

[9]We are indebted to G. Zeller for providing us with these preliminary results.

[10]Within the Rein-Sehgal model, this constant is implicitly fixed to approximately 1.2, since the Goldberger-Treiman relation is used to express the coherent π^0 production cross section in terms of the elastic $\pi^0 N \to \pi^0 N$ one.

[11]Within our model, we include these modifications by means of the consideration of the Δ-self-energy, by considering the Pauli blocking in the computation of Δ-decay width in the medium, and by using the pion wave function, $\tilde{\varphi}_\pi^*$, instead of a plane wave.

are not accounted for in the Rein-Sehgal model, and that turn out to be relevant at MiniBooNE energies.

2. The $E_\pi(1-\cos\theta_\pi) > 0.1$ GeV region and NUANCE FSI

We turn now to the region $E_\pi(1-\cos\theta_\pi) > 0.1$ GeV. Also in this region, the bulk of the discrepancies among our predictions and the MiniBooNE results can be understood in terms of the inaccuracies of the Rein-Sehgal model at low energies, as can be appreciated in the right bottom panel of Fig. 8. But here, the outgoing π^0 FSI effects, incorporated by the analysis of Ref. [18], induce some additional discrepancies. The MiniBooNE analysis relies on the Rein-Sehgal models for incoherent (resonant) [72] and coherent [9] π^0 production, which are implemented in the NUANCE event generator [73]. In the case of coherent production, the Rein-Sehgal model includes an absorption factor $F_{\rm abs}$ to effectively account for the pion wave function distortion from a plane wave (see Eq. (33)). This Glauber-type factor decreases exponentially with the pion-nucleon inelastic cross section (see Eq. 24 of Ref. [9]) and thus it neither accounts for pion absorption, which is a two nucleon mechanism, nor it does for quasielastic distortion. Quasielastic steps, induced by elastic pion-nucleon collisions and not forbidden by Pauli blocking, excite and/or break the nucleus, and are not removed by this factor $F_{\rm abs}$. This Glauber factor only removes events where the π^0 suffers an inelastic collision with a nucleon, and as a result changes its charge, or other mesons are produced in the final state.

The procedure followed in Ref. [18] to describe coherent pion production is somewhat different. They set $F_{\rm abs}$ to 1 in the Rein-Sehgal model of Ref. [9], and implement absorption as part of the FSI. In our understanding, the coherent pion production cross section cannot be calculated from a Monte Carlo cascade algorithm. This is because, by definition, the coherent production is a one step process,[12] and the quantum mechanical transition matrix element gives the amplitude probability for producing a pion outside of the nucleus, which is left unchanged. The coherent contribution should be incoherently added to that due to the inelastic channels to find out the total pion production cross section.

Nevertheless, one could still reasonably estimate the total coherent cross section from the NUANCE FSI cascade, if it would be used to eliminate from the flux of outgoing neutral pions, not only those which get absorbed or those that suffer inelastic processes, like multiple pion production, meson production or pion charge exchange, but also those that undergo quasielastic steps, induced by elastic pion-nucleon collisions, in their way out of the nucleus. However, to our knowledge, these latter events are accounted for in the MiniBooNE analysis, despite the fact that they are not coherent since the final nucleus, as a result of the secondary collisions, is not left in the ground state. We believe this is acknowledged by the authors of Ref. [18] when they say "…that rescattered events with a π^0 in the final state may be misclassified in NUANCE, as would be the case when a coherently produced π^0 rescatters elastically through a resonance." As a result of these collisions, the π^0's might change their direction and give rise to events in the NUANCE cascade at significantly larger values of θ_π. Indeed in the right bottom panel of Fig. 8, we observe significantly less events for $E_\pi(1-\cos\theta_\pi) > 0.1$ GeV when the NUANCE FSI is turned off (dashed histogram).[13] The effects below 0.1 GeV are much smaller, and in total, the change in the shape leads to a reduction of around 20% in the integrated cross section.

In our calculation of the coherent cross section, we certainly remove those secondary events by means of the optical potential employed to compute the pion wave function. The imaginary part of the pion-nucleus potential is responsible for the removal of flux of the outgoing pions on their way out of the nucleus. This imaginary part is due to pion absorption, but also to pion quasielastic steps. Hence, the use of the full optical potential will eliminate the pions which are absorbed and also those which scatter quasielastically. We might try to theoretically estimate this effect by switching off the quasielastic contribution to the pion-nucleus optical potential induced by elastic pion-nucleon collisions, and using an optical potential with an imaginary part due to absorption and inelastic channels alone. In this way, we will remove the absorbed pions and those that undergo inelastic collisions, but not those which scatter quasielastically, which will still go out of the nucleus and are accounted for by the MiniBooNE Monte Carlo generator. This was considered in the past

[12]The nomenclature here might be confusing. There exist multiple step contributions to the coherent reaction. For instance, a Δ is formed in an NC scattering; it decays with the nucleon falling back into the hole created by Δ formation; the decay π^0 creates a subsequent Δ, which in turn decays emitting a π^0 that escapes the nucleus and the associated nucleon also drops into the ground state configuration. The point we want to make here is that such contributions cannot be taken into account in a Monte Carlo cascade algorithm. This is because it would require the coherent sum of the multiple step amplitudes, while a Monte Carlo algorithm uses probabilities (cross sections). We do include these multiple step contributions within our formalism thanks to the use of a pion wave function solution of the Klein-Gordon equation, with an optical π^0-nucleus potential, instead of using a plane wave.

[13]Note that when the NUANCE FSI is turned off, besides getting rid of the unwanted quasielastic steps, pion absorption is not taken into account. However, although this latter effect produces a diminution of events, it does not significantly change the shape of the $E_\pi(1-\cos\theta_\pi)$ distribution. On the other hand, since the histogram has been rescaled down, the overall normalization is not an issue anymore. Nevertheless, we should point out that there could be some minor differences in the acceptance or cut efficiencies with respect to those used in the published histogram [18].

in the study of the pionic decay of Λ-hypernuclei [74,75], leading to moderate enhancements of the decay widths of the order of 10–15% in ^{12}C [76]. We find here similar effects, and for the MiniBooNE flux-averaged cross section, we find an enhancement of around 20% (see Table II), in good agreement with the effects observed by turning off the NUANCE FSI.

C. K2K, MiniBooNE and T2K flux-averaged cross sections

In Table II we show our predictions for the K2K [11] and MiniBooNE [18] flux-averaged cross sections as well as for the future T2K experiment. In Fig. 9, we show some results for K2K and MiniBooNE experiments. In all cases, we normalize the neutrino or antineutrino flux ϕ to one. In principle, we would like to compute the corresponding convolution with the neutrino or antineutrino flux

$$\bar{\sigma} = \int_{E^i_{\rm low}}^{E^i_{\rm high}} dE \phi^i(E)\sigma(E), \qquad i = \text{K2K, MiniBooNE, T2K} \tag{35}$$

with $E^i_{\rm low}$, $E^i_{\rm high}$ the lower and upper flux limits, and $\sigma(E)$ the corresponding CC/NC muon/electron neutrino/antineutrino-induced nuclear coherent cross section, as a function of the neutrino/antineutrino energy.[14] In practice, the predictions of our model become less reliable when the energy increases, since the model neglects all resonances above the Δ(1232). Sophisticated recent calculations, as those of Refs. [30–32], suffer from exactly the same limitation. That is the reason why we have set up a maximum neutrino energy ($E^i_{\rm max}$) in the convolution, and approximated

$$\bar{\sigma} \approx \frac{\int_{E^i_{\rm low}}^{E^i_{\rm max}} dE \phi^i(E)\sigma(E)}{\int_{E^i_{\rm low}}^{E^i_{\rm max}} dE \phi^i(E)} \tag{36}$$

where we fix the upper limit in the integration (neglecting the long tail of the neutrino fluxes) to $E_{\rm max} = 1.45$ and 1.34 GeV for CC and NC muon neutrino/antineutrino driven processes, respectively. The phase space for the fifth differential $\frac{d^5\sigma}{d\Omega(\hat{k}')dE'd\Omega(\hat{k}_\pi)}$ cross section, up to irrelevant constants, is determined by $|\vec{k}'||\vec{k}_\pi|$ (see Eqs. (2), (4), (19), and (20)). For CC processes, for instance, and muon neutrino energies of around 1.45 GeV, the phase space peaks at pion energies of around 730 MeV, which leads, neglecting the nucleon momentum, to πN invariant masses below 1.5 GeV. Up to these energies, one can reasonably assume Δ(1232) dominance.

[14]Note that the cross section trivially vanishes for neutrino/antineutrino energies below the pion production threshold, which obviously is different for CC and NC driven processes because of the final lepton mass.

In the case of the K2K experiment a threshold of 450 MeV for muon momentum was imposed as an additional selection criterion [11]. We have implemented this cut also here, and in that case we have been able to go up to $E^{\rm CC,K2K}_{\rm max} = 1.8$ GeV. In these circumstances, we still cover about 90% of the total flux in most of the cases. For the T2K antineutrino flux, we cover just about 65% of the total spectrum, and therefore our results for the convoluted cross sections are less reliable.

For neutrino energies above 1 GeV, and though the Δ contribution plays a central role in pion production [72], one should bear in mind that other resonances could certainly be also important. This would affect the results presented in Table II and Fig. 9. Taking into account that the T2K and MiniBooNE fluxes peak at neutrino energies of around 0.6–0.7 GeV, where the Δ resonance contribution is much more dominant, it is reasonable to expect corrections (higher cross sections) of around 20–30% to our results for these two experiments. Certainly, the corrections could be larger for the K2K case, since in that case the neutrino energy spectrum peaks at higher energies, around 1.2 GeV.

We see that our prediction, subject to some uncertainties, lies well below the K2K upper bound, mainly thanks to the use of a low value for $C_5^A(0)$, while we predict a NC MiniBooNE cross section notably smaller than that given in the PhD thesis of J. L. Raaf [77]. However, this latter value should be taken with extreme caution. It was obtained from a preliminary analysis that since then has been notably improved. Moreover, the MiniBooNE Collaboration has not given an official value for the total coherent cross section yet, and only the ratio coherent/(coherent + incoherent) has been presented [18]. Nevertheless, as we have discussed at length, we believe the MiniBooNE analysis might overestimate this ratio, not only because some of the π^0's which undergo FSI collisions are accounted for as coherent events instead of being removed, but more importantly because the Rein-Sehgal model predicts an incorrect (wider) $E_\pi(1-\cos\theta_\pi)$ shape for coherent π^0's. The first of the effects produces an enhancement of the coherent cross section of the order of 20% (see the MiniBooNE NC* entry in the table), while it is much more difficult to quantify the second of the effects. This is because, in addition to the variation of the integrated area, it might produce a possible mismatch between the absolute normalization of the background, coherent and incoherent yields in the MiniBooNE analysis. To finish this discussion, we would like to point out that the K2K cross section and the value quoted in Ref. [77] seem somehow incompatible with the approximate relation $\sigma_{\rm CC} \approx 2\sigma_{\rm NC}$, expected from Δ-dominance and neglecting finite muon mass effects (see discussion at the end of Sec. III).

Our predictions are about 20–30% smaller than those obtained in Ref. [32] from model II, which uses our value $C_5^A(0) \approx 0.9$. This discrepancy is due to different facts: the

TABLE II. NC/CC muon neutrino and antineutrino coherent pion production total cross sections for K2K, MiniBooNE and T2K experiments. In the case of CC K2K, the experimental threshold for the muon momentum $|\vec{k}'| > 450$ MeV is taken into account. To convert the cross section ratio given in [11] into a coherent cross section (K2K), we use the value of 1.07×10^{-38} cm^2/nucleon for the total CC cross section, as quoted in [11]. For the MiniBooNE NC* entry, we present our results when an optical pion-nucleus potential with an imaginary part due to absorption and inelastic channels alone is used to compute the distortion of the outgoing pion (see text for more details). The absolute NC π^0 coherent cross section quoted in the PhD thesis of Ref. [77] should be taken with extreme caution, since in the published paper (Ref. [18]) it is not given. There, it is quoted the ratio of the sum of the NC coherent and diffractive modes over all exclusive NC π^0 production at MiniBooNE. Some details on the flux convolution are compiled in the last three columns.

Reaction	Experiment	$\bar{\sigma}$ [10^{-40} cm^2]	$\sigma_{\rm exp}$ [10^{-40} cm^2]	$E^i_{\rm max}$ [GeV]	$\int_{E^i_{\rm low}}^{E^i_{\rm max}} dE\phi^i(E)\sigma(E)$ [10^{-40} cm^2]	$\int_{E^i_{\rm low}}^{E^i_{\rm max}} dE\phi^i(E)$
CC $\nu_\mu + {}^{12}$C	K2K	4.68	$<$7.7 [11]	1.80	3.84	0.82
CC $\nu_\mu + {}^{12}$C	MiniBooNE	2.99		1.45	2.78	0.93
CC $\nu_\mu + {}^{12}$C	T2K	2.57		1.45	2.34	0.91
CC $\nu_\mu + {}^{16}$O	T2K	3.03		1.45	2.76	0.91
NC $\nu_\mu + {}^{12}$C	MiniBooNE	1.97	$7.7 \pm 1.6 \pm 3.6$ [77]	1.34	1.75	0.89
NC* $\nu_\mu + {}^{12}$C	MiniBooNE	2.38*	$7.7 \pm 1.6 \pm 3.6$ [77]	1.34	2.12*	0.89
NC $\nu_\mu + {}^{12}$C	T2K	1.82		1.34	1.64	0.90
NC $\nu_\mu + {}^{16}$O	T2K	2.27		1.35	2.04	0.90
CC $\nu_\mu + {}^{12}$C	T2K	2.12		1.45	1.42	0.67
NC $\nu_\mu + {}^{12}$C	T2K	1.50		1.34	0.96	0.64

existence of some numerical inaccuracies affecting the results of Refs. [31,32], the inclusion of the nonzero momenta in the nucleon spinors, different ranges in the flux convolution, etc.

For the future T2K experiment, we get cross sections of the order $2 - 2.6 \times 10^{-40}$ cm^2 in carbon and about $2.3 - 3.0 \times 10^{-40}$ cm^2 in oxygen, considerably smaller than those predicted by the Rein-Sehgal model.

The SciBooNE Collaboration has recently set 90% confidence level upper limits on the cross section ratio of CC coherent pion production to the total CC cross section at 0.67×10^{-2} at mean neutrino energy 1.1 GeV and 1.36×10^{-2} at mean neutrino energy 2.2 GeV [15]. If we use a value of 1.05×10^{-38} cm^2/nucleon for the total CC cross section, as quoted in [15], the SciBooNE upper limit for the ratio will transform in a upper bound of about 8×10^{-40} cm^2 for the coherent cross section at 1.1 GeV. At 1.1 GeV, our prediction for the CC coherent pion production cross section in carbon is 5.7×10^{-40} cm^2 (see points in the left panel of Fig. 9), which is totally compatible with

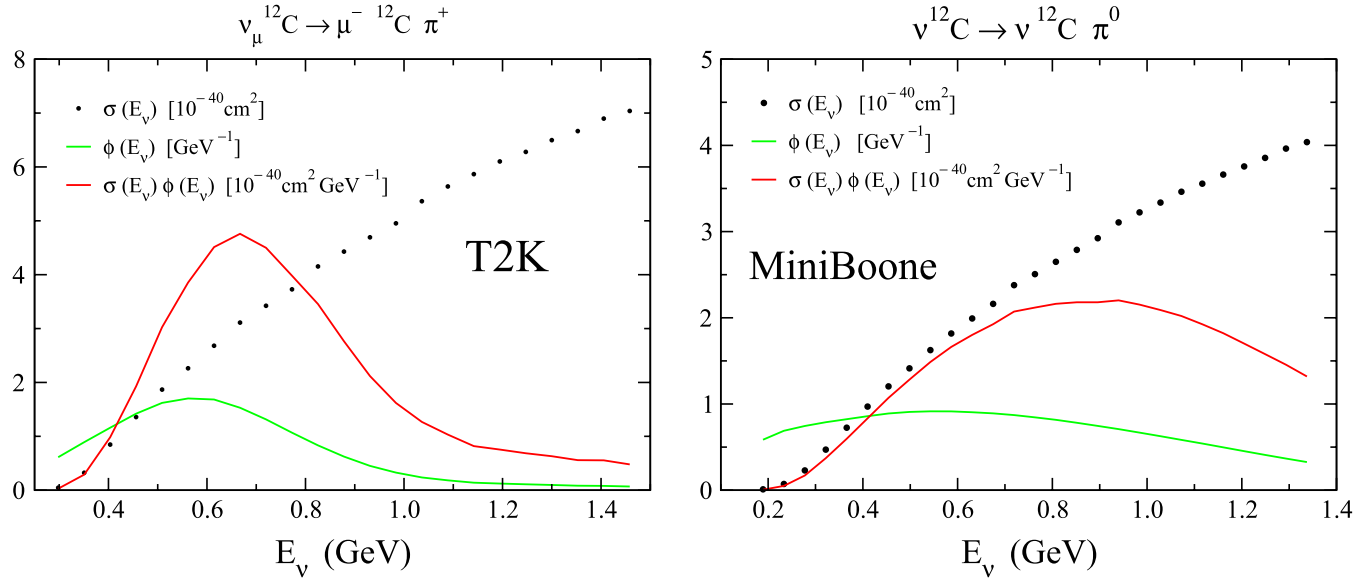

FIG. 9 (color online). CC (left) and NC (right) coherent pion production cross sections in carbon. We also show predictions multiplied by the T2K (left) and MiniBooNE (right) ν_μ neutrino energy spectra. In the region of neutrino energies around 0.6 GeV, the lower curves stand for the T2K and MiniBooNE ν_μ fluxes normalized to one.

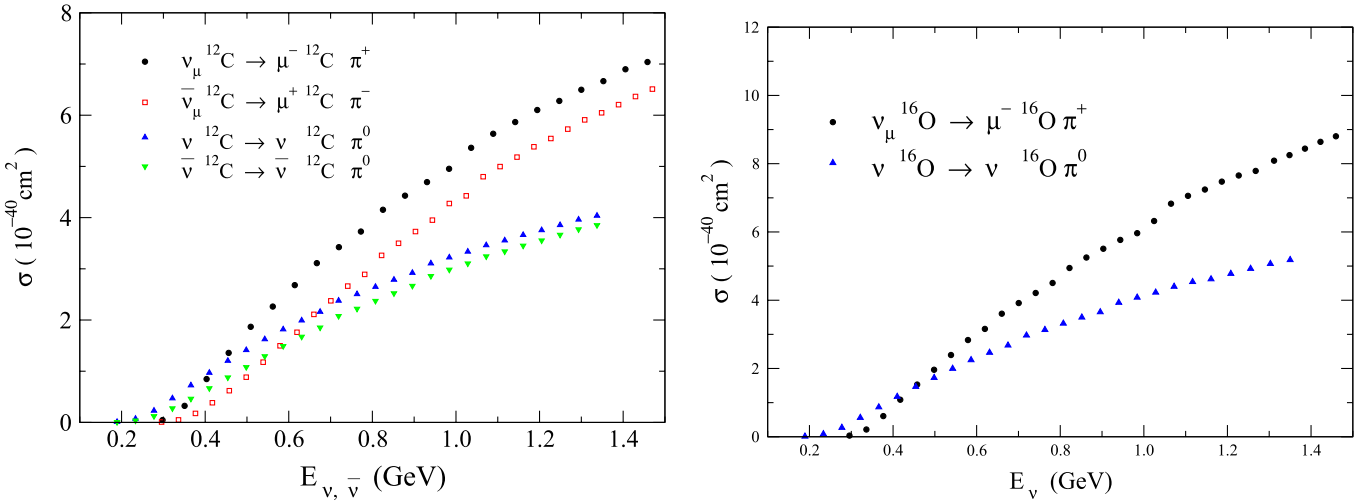

FIG. 10 (color online). Muon neutrino/antineutrino CC and NC coherent pion production off nuclei from carbon (left) and oxygen (right) targets as a function of the neutrino/antineutrino energy.

the SciBooNE bound. However, according to the Rein-Sehgal model [9,12] implemented in the SciBooNE simulation, the cross section ratio of CC coherent pion production to the total CC cross section is calculated to be 2.04×10^{-2} in Ref. [15]. The SciBooNE limits correspond to 33% and 67% of the Rein-Sehgal model prediction at 1.1 GeV and 2.2 GeV, respectively [15]. From our discussion in Sec. IV B (see last paragraph in Sec. IV B 1), we easily understand why the Rein-Sehgal model overestimates the coherent cross sections by a large factor at neutrino energies around 1 GeV (approximately a factor of 2 because of the value[15] of $C_5^A(0)$, and approximately another factor of 2 because of the $t = 0$ approximation in the amplitudes, in addition to all sorts of in-nuclear-medium effects, like pion absorption or modification of the elementary $\pi N \rightarrow \pi N$ cross section in the medium, which are not accounted for in the Rein-Sehgal model). We also understand why at the higher neutrino energy of 2.2 GeV the Rein-Sehgal model works better, since the larger the energy, the better the $t = 0$ approximation in the amplitudes and the smaller the nuclear effects become. Note also that at 2.2 GeV we expect heavier resonances than the $\Delta(1232)$ to play an important role, and thus the issue of the value of $C_5^A(0)$ is less relevant.

To conclude this section, in Fig. 10 we show muon neutrino/antineutrino CC and NC coherent pion production off carbon and oxygen targets. We see that both for CC and NC driven processes, the ratio of neutrino over antineutrino cross sections approaches one as the neutrino energy increases. This is due to the nuclear form factor which reduces the vector contribution to the amplitudes (and therefore the interference between the vector and the axial parts) as the neutrino energy increases. Besides, and as a consequence of the nuclear form factor and other nuclear in-medium effects, we also see that cross sections do not scale as A^2, A being the nuclear mass number, as expected from a coherent reaction. This is in good agreement with the findings of Refs. [9,31]. Indeed at 1 GeV, oxygen and carbon cross sections turn out to be in a proportion of around 6 to 5, instead of 1.8 to 1, as it would be deduced from an A^2-type scaling law. Finally, we observe sizable corrections to the approximate relation $\sigma_{CC} \approx 2\sigma_{NC}$ for these two isoscalar nuclei in the whole range of neutrino/antineutrino energies examined in this work. As pointed out in Refs. [12,14], this is greatly due to the finite muon mass, and thus the deviations are dramatic at low neutrino energies. In any case, these corrections cannot account for the apparent incompatibility among the CC K2K cross section and the NC value quoted in Ref. [77], mentioned above.

[15]Note, however that, $C_5^A(0)$ will partially cancel out in the ratios measured by the SciBooNE Collaboration.

V. CONCLUSIONS

We have developed a model for neutrino/antineutrino CC and NC coherent pion production off nuclei which is based on a microscopic model for neutrino/antineutrino-induced one-pion production off the nucleon derived in Ref. [33]. The model of Ref. [33] includes the dominant Δ production mechanism, but it also takes into account background terms required by chiral symmetry. In its application to coherent production we have further taken into account the main nuclear effects expected to be important in reactions off nuclei. While the model presented here is similar to the one in Refs. [31,32], we have improved on that calculation by taking consistently into account the nucleon motion, and by using a more sophisticated pion optical potential. The consideration of the nucleon motion increases the cross section by a non-negligible amount, while Coulomb effects on the emission of charged pions

lead to small changes in the cross section. Moreover, we have corrected for some numerical inaccuracies [52] (of the order of 20% in the total cross section, and larger at the peak of the $d\sigma/dk_\pi$ differential distribution) that affected the calculations carried out in Refs. [31,32].

In agreement with Refs. [31,32], we find a strong reduction of the cross section, mainly due to the modification of the Δ self-energy in the nuclear medium, and a shift to lower energies of the outgoing pion distribution due to the final pion distortion. The angular distributions of both pion and muons with respect to the incoming ν_μ direction are forward peaked due to the nuclear form factor. While the muon angular distribution profile is almost unaffected by nuclear corrections, in the pion case, part of the strength is shifted to larger angles due to the distortion of the final pion wave function. Nonresonant terms, which turned out to be very important at the nucleon level [33],[16] give small contributions to the coherent pion production off isospin symmetric nuclei. This leads us to find coherent pion production cross sections around a factor of 2 smaller than most of those previously published.

We have also performed a detailed discussion of the MiniBooNE results of Ref. [18] and the analysis performed there to identify NC coherent π^0 events. We have shown that the Rein-Sehgal model used in this analysis is not accurate enough in this case. This is because the MiniBooNE flux mainly consists of neutrinos below 2 GeV, and for such low neutrino energies, the corrections to the outgoing pion angular dependence predicted by the Rein-Sehgal model become quite important. As a consequence, the Rein-Sehgal model leads to distributions notably wider and integrated cross sections much larger than those predicted in this work. Finally, we have predicted muon neutrino/antineutrino CC and NC coherent pion production off carbon and oxygen up to neutrino energies of the order of 1.4 GeV, and convoluted those cross sections with the K2K, T2K and MiniBooNE fluxes. Our cross sections are considerably smaller than those predicted by the Rein-Sehgal model.

We expect the present model to provide accurate coherent pion production total and differential cross sections in the first resonance region, where the $\Delta(1232)$ plays a relevant role. This energy region is very important for the analysis of present and forthcoming neutrino oscillation experiments for which good and reliable theoretical calculations are needed.

[16]Their inclusion made it necessary to reduce the nucleon-to-Δ resonance axial coupling.

ACKNOWLEDGMENTS

We warmly thank L. Alvarez-Ruso, G. T. Garvey, F. Sanchez, M. Sorel, M. J. Vicente-Vacas and G. Zeller for useful discussions. This research was supported by DGI and FEDER funds, under Contract Nos. FIS2005-00810, FIS2006-03438, FPA2007-65748, and the Spanish Consolider-Ingenio 2010 Programme CPAN (CSD2007-00042), by Junta de Andalucía and Junta de Castilla y León under Contract Nos. FQM0225 and SA016A07, and it is part of the EU integrated infrastructure initiative Hadron Physics Project under Contract No. RII3-CT-2004-506078.

[1] A. A. Aguilar-Arevalo *et al.* (MiniBooNE Collaboration), Phys. Rev. Lett. **98**, 231801 (2007).
[2] K. Hiraide (SciBooNE Collaboration), Nucl. Phys. B, Proc. Suppl. **159**, 85 (2006).
[3] P. Marage *et al.* (BEBC WA59 Collaboration), Z. Phys. C **31**, 191 (1986).
[4] H. J. Grabosch *et al.* (SKAT Collaboration), Z. Phys. C **31**, 203 (1986).
[5] P. P. Allport *et al.* (BEBC WA59 Collaboration), Z. Phys. C **43**, 523 (1989).
[6] M. Aderholz *et al.* (E632 Collaboration), Phys. Rev. Lett. **63**, 2349 (1989).
[7] P. Vilain *et al.* (CHARM-II Collaboration), Phys. Lett. B **313**, 267 (1993).
[8] S. Willocq *et al.* (E632 Collaboration), Phys. Rev. D **47**, 2661 (1993).
[9] D. Rein and L. M. Sehgal, Nucl. Phys. **B223**, 29 (1983).
[10] S. L. Adler, Phys. Rev. **135**, B963 (1964).
[11] M. Hasegawa *et al.* (K2K Collaboration), Phys. Rev. Lett. **95**, 252301 (2005).
[12] D. Rein and L. M. Sehgal, Phys. Lett. B **657**, 207 (2007).
[13] S. L. Adler, arXiV:hep-ph/0505177.
[14] Ch. Berger and L. M. Sehgal, Phys. Rev. D **76**, 113004 (2007); **77**, 059901(E) (2008).
[15] K. Hiraide *et al.* (SciBooNE Collaboration), arXiv:0811.0369.
[16] H. Faissner *et al.*, Phys. Lett. B **125**, 230 (1983).
[17] E. Isiksal, D. Rein, and J. G. Morfin, Phys. Rev. Lett. **52**, 1096 (1984).
[18] A. A. Aguilar-Arevalo *et al.* (MiniBooNE Collaboration), Phys. Lett. B **664**, 41 (2008).
[19] O. Nachtmann, Nucl. Phys. **B22**, 385 (1970).
[20] J. S. Bell, Phys. Rev. Lett. **13**, 57 (1964).
[21] A. Pais and S. B. Treiman, Phys. Rev. D **9**, 1459 (1974).
[22] K. S. Lackner, Nucl. Phys. **B153**, 526 (1979).
[23] A. A. Belkov and B. Z. Kopeliovich, Yad. Fiz. **46**, 874 (1987); [Sov. J. Nucl. Phys. **46**, 499 (1987)].
[24] B. Z. Kopeliovich, Nucl. Phys. B, Proc. Suppl. **139**, 219 (2005).
[25] S. S. Gershtein, Yu. Y. Komachenko, and M. Y. Khlopov,

Sov. J. Nucl. Phys. **32**, 861 (1980).
[26] Yu. Y. Komachenko and M. Y. Khlopov, Yad. Fiz. **45**, 467 (1987).
[27] E. A. Paschos, A. Kartavtsev, and G. J. Gounaris, Phys. Rev. D **74**, 054007 (2006).
[28] H. C. Kim, S. Schramm, and C. J. Horowitz, Phys. Rev. C **53**, 3131 (1996).
[29] N. G. Kelkar, E. Oset, and P. Fernandez de Cordoba, Phys. Rev. C **55**, 1964 (1997).
[30] S. K. Singh, M. Sajjad Athar, and S. Ahmad, Phys. Rev. Lett. **96**, 241801 (2006).
[31] L. Alvarez-Ruso, L. S. Geng, S. Hirenzaki, and M. J. Vicente Vacas, Phys. Rev. C **75**, 055501 (2007).
[32] L. Alvarez-Ruso, L. S. Geng, and M. J. Vicente Vacas, Phys. Rev. C **76**, 068501 (2007).
[33] E. Hernandez, J. Nieves, and M. Valverde, Phys. Rev. D **76**, 033005 (2007).
[34] A. Gil, J. Nieves, and E. Oset, Nucl. Phys. **A627**, 543 (1997).
[35] S. L. Adler, Ann. Phys. (N.Y.) **50**, 189 (1968).
[36] C. H. Llewellyn Smith, Phys. Rep. **3**, 261 (1972).
[37] P. A. Schreiner and F. Von Hippel, Phys. Rev. Lett. **30**, 339 (1973).
[38] L. Alvarez-Ruso, S. K. Singh, and M. J. Vicente Vacas, Phys. Rev. C **57**, 2693 (1998).
[39] L. Alvarez-Ruso, S. K. Singh, and M. J. Vicente Vacas, Phys. Rev. C **59**, 3386 (1999).
[40] O. Lalakulich and E. A. Paschos, Phys. Rev. D **71**, 074003 (2005).
[41] T. Leitner, L. Alvarez-Ruso, and U. Mosel, Phys. Rev. C **73**, 065502 (2006).
[42] E. A. Paschos, J. Y. Yu, and M. Sakuda, Phys. Rev. D **69**, 014013 (2004).
[43] O. Lalakulich, E. A. Paschos, and G. Piranishvili, Phys. Rev. D **74**, 014009 (2006).
[44] G. L. Fogli and G. Nardulli, Nucl. Phys. **B160**, 116 (1979).
[45] G. L. Fogli and G. Nardulli, Nucl. Phys. **B165**, 162 (1980).
[46] T. Sato, D. Uno, and T. S. H. Lee, Phys. Rev. C **67**, 065201 (2003).
[47] S. J. Barish *et al.*, Phys. Rev. D **19**, 2521 (1979).
[48] G. M. Radecky *et al.*, Phys. Rev. D **25**, 1161 (1982); **26**, 3297(E) (1982).
[49] C. Alexandrou, T. Leontiou, J. W. Negele, and A. Tsapalis, Phys. Rev. Lett. **98**, 052003 (2007).
[50] D. Barquilla-Cano, A. J. Buchmann, and E. Hernandez, Phys. Rev. C **75**, 065203 (2007); **77**, 019903(E) (2008).
[51] K. M. Graczyk and J. T. Sobczyk, Phys. Rev. D **77**, 053001 (2008).
[52] L. Alvarez-Ruso, L. S. Geng, and M. J. Vicente Vacas private communication.
[53] I. Kato (K2K and T2K Collaborations), Nucl. Phys. B, Proc. Suppl. **168**, 199 (2007).
[54] R. C. Carrasco, J. Nieves, and E. Oset, Nucl. Phys. **A565**, 797 (1993).
[55] S. Hirenzaki, J. Nieves, E. Oset, and M. J. Vicente-Vacas, Phys. Lett. B **304**, 198 (1993).
[56] P. Fernandez de Cordoba, J. Nieves, E. Oset, and M. J. Vicente-Vacas, Phys. Lett. B **319**, 416 (1993).
[57] S. Boffi, L. Bracci, and P. Christillin, Nuovo Cimento A **104**, 843 (1991).
[58] W. Peters, H. Lenske, and U. Mosel, Nucl. Phys. **A640**, 89 (1998).
[59] D. Drechsel, L. Tiator, S. S. Kamalov, and S. N. Yang, Nucl. Phys. **A660**, 423 (1999).
[60] M. Hirata, J. H. Koch, E. J. Moniz, and F. Lenz, Ann. Phys. (N.Y.) **120**, 205 (1979).
[61] E. Oset, H. Toki, and W. Weise, Phys. Rep. **83**, 281 (1982).
[62] E. Oset and L. L. Salcedo, Nucl. Phys. **A468**, 631 (1987).
[63] J. Nieves, E. Oset, and C. Garcia-Recio, Nucl. Phys. **A554**, 509 (1993).
[64] J. Nieves, E. Oset, and C. Garcia-Recio, Nucl. Phys. **A554**, 554 (1993).
[65] J. Nieves, M. Valverde, and M. J. Vicente Vacas, Phys. Rev. C **73**, 025504 (2006).
[66] C. W. De Jager, H. De Vries, and C. De Vries, At. Data Nucl. Data Tables **14**, 479 (1974).
[67] J. W. Negele and D. Vautherin, Phys. Rev. C **11**, 1031 (1975), and references therein.
[68] C. Garcia-Recio, J. Nieves, and E. Oset, Nucl. Phys. **A547**, 473 (1992).
[69] T. Kitagaki *et al.*, Phys. Rev. D **34**, 2554 (1986).
[70] G. Zeller (private communication).
[71] J. Link, "Fifth International Workshop on Neutrino-Nucleus Interaction in the Few GeV Region (Nuint07)," Fermilab, Batavia, Illinois, USA., http://conferences.fnal.gov/nuint07/.
[72] D. Rein and L. M. Sehgal, Ann. Phys. (N.Y.) **133**, 79 (1981).
[73] E. A. Hawker, Nucl. Phys. B, Proc. Suppl. **139**, 260 (2005).
[74] J. Nieves and E. Oset, Phys. Rev. C **47**, 1478 (1993).
[75] U. Straub, J. Nieves, A. Faessler, and E. Oset, Nucl. Phys. **A556**, 531 (1993).
[76] C. Albertus, J. E. Amaro, and J. Nieves, Phys. Rev. C **67**, 034604 (2003).
[77] J. L. Raaf, PhD thesis, University of Cincinnati [Institution Report No. FERMILAB-THESIS-2007-20, 2005].